Green hybrid composites from cellulose nanocrystal

4

Shahab Kashani Rahimi and Joshua U. Otaigbe
School of Polymers and High Performance Materials, The University of Southern Mississippi, Hattiesburg, MS, United States

Chapter Outline

4.1 Introduction

Over the past decade, tremendous research and development efforts have been focused on cellulose nanomaterials both as reinforcing and functional additives for polymer composite application as well as building block for development of novel functional materials. These efforts are motivated by a number of enhanced benefits of cellulosic fibers such as natural abundance and availability, inherent biorenewability and

Hybrid Polymer Composite Materials: Structure and Chemistry. DOI: http://dx.doi.org/10.1016/B978-0-08-100791-4.00004-5
Copyright © 2017 Elsevier Ltd. All rights reserved.

sustainability, exceptional structural and mechanical properties, low cost, low density, and biodegradability. One of the main challenges in using natural fibers as reinforcing components of polymer composites is the variation of properties based on their original climatic conditions, species, age, and spatial distribution of properties within the lingocellulosic fibers. One approach to avoid the negative impact of this variation of properties is to eliminate the hierarchical structure inherent to cellulosic fibers by removing the fiber constituents to extract the highly rigid and crystalline core of the fibrillar assembly known as cellulose nanocrystals (CNCs) or cellulose whiskers. These nanoscale cellulosic moieties have attracted a great level of academic and industrial attention not only because of their superior structural and mechanical properties (as will be discussed in this review) but also due to their nanoscale dimensions, high surface area, and natural abundance of their source cellulosic material which makes them superior alternatives to conventional nanoadditives and fibers such as silicates, glass, and inorganic nanomaterials traditionally used in composites applications. As an example, taking the density of CNCs to be at approximately 1.5 g cm^{-3} (cf. 2.6−3 g cm^{-3} for inorganic clays), a significant weight reduction of the final nanocomposite material is expected to be obtained simply by replacing clays with CNCs in the nanocomposite [1].

In fact, CNCs or cellulose whiskers are the highly crystalline core fraction of cellulosic fibers where other components such as lignin, hemicellulose, proteins, extractives, and paracrystalline interfibrillar regions are removed in the extraction process, leaving behind the tightly packed rod-shape defect-free cellulose fraction that are held together by strong hydrogen bonding of cellulose macromolecules. The hierarchical structure of cellulose fiber is shown in Fig. 4.1 [2].

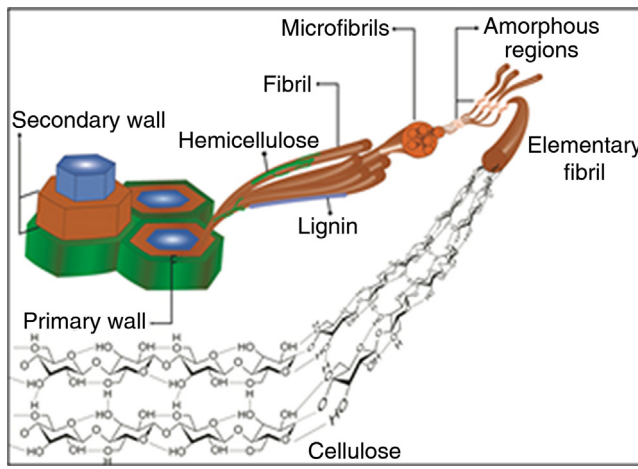

Figure 4.1 Hierarchical structure of cellulose derived from wood/plants.
Reproduced from Ref. [2]: {2015} {John Rojas, Mauricio Bedoya and Yhors Ciro}. Originally published in *Current Trends in the Production of Cellulose Nanoparticles and Nanocomposites for Biomedical Applications, Cellulose − Fundamental Aspects and Current Trends, Dr. Matheus Poletto (Ed.), InTech*, under CC BY 3.0 license. Available from: DOI: 10.5772/61334.

These nanocrystals possess exceptional mechanical properties with axial Young's modulus reported to be as high as 160 GPa, a value surpassing that of Kevlar and steel [3].

Cellulose macromolecule is comprised of rigid linear chain of ringed glucose units that are formed by a covalent link of β 1−4 glucosidic bond between the anhydroglucose rings ($C_6H_{10}O_5$) [4]. Strong intermolecular hydrogen bonding via hydroxyl units of the glucose and oxygen of neighboring ring unit stabilizes the links, resulting in linear chain configuration with chair conformation [5]. This strong hydrogen bonding is the basis of formation of this elementary fibrillar structure which further aggregates into microfibrillar arrangement. Depending on the nature of the natural cellulose fiber, the arrangement of the fibrils and the degree of polymerization of the cellulose (or its length) vary among different species and sources. The microfibrils are the basic building blocks of the wood/plant cell wall. These fibrils are composed of cellulose crystallites that are connected via amorphous regions which are further wrapped in a polyglucosan material and hemicellulose. These microfibrils are held together via a matrix of lignin, proteins, and extractives. Therefore, certain processes have been developed in order to isolate the highly crystalline cellulose in the core of the fibrils. In this chapter, a survey is provided that covers previous research efforts together with some recent developments in the area of polymer/CNC nanocomposites and properties of CNCs, processing, and properties of CNC-based nanocomposite materials.

4.2 Preparation of cellulose nanocrystals: sources and extraction methods

CNCs are usually prepared using a number of different methods such as acid hydrolysis, mechanical process, enzymatic synthesis, and a recent approach using ionic liquids (ILs) [5]. Normally, in a typical process, a two-stage procedure is followed which depends on the cellulose source material. The first step involves the removal of polyglucosan components (except the cellulose fibrils), and the second stage involves extraction of the nanocrystalline regions. Specifically, lingocellulosic fibers are first chemically treated to remove the lignin, hemicellulose, and extractives. A more recent approach that has been used in a number of studies is based on steam explosion technology [6,7] to remove the lignin and hemicellulosic portions of the biomass where typically, the lingocellulosic fibers are subjected to high-pressure steam at a pressure of around 15 bars for a certain amount of time (usually less than 20 min) at temperature range of 220−270°C. The fibers are then immediately exposed to atmospheric pressure by opening the chamber which causes the lignin/hemicellulose fractions to explode. These fractions can then be removed by extraction leaving the highly crystalline cellulose fibrils for further processing of CNC extraction.

In the case of CNCs derived from the tunicate [8], the mantle is isolated from the animal followed by removal of the encapsulating protein components surrounding the microfibrils. In the case of bacterial and enzymatic cellulose production, after the cellulose microfibrils are cultivated, the walls and other components are removed

by washing with alkaline solutions [9,10]. After the removal of the matrix material in the cellulose source, the second stage of the production of CNCs usually involves a number of treatments that include acid hydrolysis, mechanical process, and a bacterial/enzymatic treatment that will be described later in detail in this section.

One of the major factors that dictates the final morphology and structure of the CNCs is the source material used to isolate the CNCs. Various cellulosic materials have been used to prepare the CNCs including wood fibers such as bleached softwood [11] and sugar beet pulp [12], cotton fibers [13], plant fibers such as flax [14], sisal [15], ramie [16], and hemp fibers [17]. In addition, the major nonplant/wood-based sources are various types of bacteria [10] as well as tunicate [8]. Typical CNCs are rod-like whiskers with lengths of 25−1000 nm and diameters of 4−50 nm. It has been shown that the CNCs obtained from tunicate and bacterial growth method have typically larger lengths due to the higher amount of crystalline fraction in the cellulosic part of these materials [18]. For example, De Souza Lima *et al.* [19] reported a length value of 1160 nm and a diameter of 16 nm for whiskers obtained from tunicate giving an aspect ratio of 72.5 while the whiskers obtained from cotton had a length of 255 nm and diameter of 15 nm with an aspect ratio of 17. Fig. 4.2 depicts Transmission Electron Microscope (TEM) images of typical morphology of the CNCs obtained from various sources. A brief review of the main approaches to fabricate CNCs is discussed in the following sections.

4.2.1 Cellulose nanocrystals from acid hydrolysis

Sulfuric acid hydrolysis is the most common method for fabrication of CNCs [5,6]. In a typical process, the cellulose starting material (i.e., after first stage of removal of the matrix containing the crystalline regions in the fiber) is suspended in de-ionized (DI)

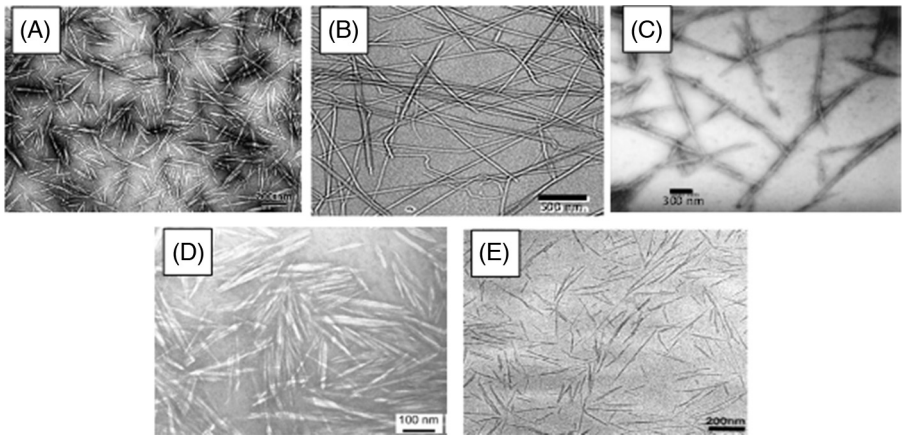

Figure 4.2 TEM images of cellulose nanocrystals extracted from (A) ramie fiber, (B) Tunicate, (C) Bacteria, (D) cotton, and (E) from sugar beet.
Images reproduced from Refs. [8,12,13,20,21] respectively with permissions from Royal Society of Chemistry, Springer and American Chemical Society.

water followed by addition of sulfuric acid at prescribed composition. Then, the reaction continues for a set amount of time at a fixed temperature. The final mixture is quenched using ice cubes, filtered or centrifuged, and dialyzed against water until a neutral pH is achieved [22]. The purpose of the acid hydrolysis process is to remove the amorphous or paracrystalline regions surrounding the highly crystalline cores of the cellulose fibrils to leave the CNCs that are more resistant toward acidic medium in the final mixture. Sulfuric acid hydrolysis results in surface-negative charges (sulfonate groups) that are responsible for colloidal stability of CNCs in aqueous solution at the price of reducing the thermal stability. A number of extensive studies have been carried out to investigate the effect of acid hydrolysis parameters such as time, temperature, and concentration of acid. For example, Dong *et al.* [23] found that a concentration of 64% (w/v) with a liquor ratio of 1:8.75 with the reaction conditions of 1 h at 45°C and ultrasonic treatment time of 5 min result in a suspension with anisotropic behavior above 4.5% (w/v).

In a comprehensive study by Bondeson *et al.* [24], the yield of the hydrolysis process as well as the particle polydispersity was examined and the obtained results correlated to hydrolysis conditions. Their results indicated that particles with an average length between 200 nm and 400 nm and diameter of less than 10 nm with a yield of 30% could be achieved with a reaction time of 2 h while longer reaction times decreased the CNC length (via depolymerization of cellulose) and increased surface-negative charge. In a systematic study by Hamad *et al.* [25], it was found that a temperature of 65°C with shorter reaction times of about 5 min resulted in the highest CNC yield of 38%. In another study [26], the effect of hydrolysis temperature on preparation of CNCs obtained from cotton fibers was investigated. Using a fixed reaction time of 30 min and sulfuric acid concentration of 65%, the authors showed that by incremental increase in temperature from 45 to 72°C, the length of the crystals reduced from 141 to 105 nm while the polydispersity of crystal size increased from 1.15 to 1.21 indicating a more nonhomogenous hydrolysis process at elevated temperatures. Interestingly, Beck-Candanedo *et al.* [11] in a study of the effect of sulfuric acid hydrolysis time and acid-to-pulp ratio on dimensions of CNCs obtained from black spruce wood pulp showed that acid hydrolysis at longer reaction times produced shorter nanocrystals with lower size distribution (or polydispersity). The effect of acid-to-pulp ratio was found to be inversely related to the nanocrystal dimension, implying that higher acid-to-pulp weight ratio results in formation of smaller crystals. The effect of acid-to-pulp ratio was found to be dependent on the retain time in such a way that the effect of acid-to-pulp ratio is more pronounced at shorter reaction time.

In an effort to reduce the polydispersity of the nanocrystals obtained by acid hydrolysis, differential centrifugation [27], and ultracentrifugation [28], methods have been adopted. Bai *et al.* [27] used a multistep centrifugation process with stepwise incremental increase in the centrifugal speed to separate various fractions of CNC from the suspension at different velocities. It was found that smaller nanocrystal fractions could be separated at higher centrifugal speeds while each fraction at each speed showed a narrow-size distribution.

In addition to sulfuric acid, a number of other mineral acids have also been used to prepare CNCs by the hydrolysis process. Yu *et al.* [29] studied the effect of hydrochloric acid hydrolysis parameters in preparation of CNCs. The optimized conditions to achieve highest yield and smallest diameter were reported to be a reaction time of 3 h at 110°C with acid-to-pulp ratio of 60 ml g^{-1}. Under these conditions, the CNC production yield from cotton and wood pulp material was 85% and 81%, respectively. In addition, it was found in the same study that the HCl-extracted nanocrystals improved thermal stability compared with that of the samples prepared by sulfuric acid hydrolysis, as well as, produced relatively narrower size distribution of the CNCs. However, one of the major disadvantages of extraction of CNC with hydrochloric acid is the lack of surface charge after the treatment process that results in significant flocculation and aggregation of whiskers and poor dispensability [30]. This characteristic is opposite to that of the treatment with sulfuric acid hydrolysis as the sulfate anions on the surface of CNC provide colloidal stability in aqueous medium. As shown in AFM images of Fig. 4.3, it is clearly seen that a cast film of the dispersion of CNC prepared from sulfuric acid hydrolysis shows a much better dispersion of whiskers compared to an aggregated structure obtained from hydrochloric acid hydrolysis method. In a series of studies by Wang *et al.* [32,33], a mixture of sulfuric and hydrochloric acid was used under ultrasonic treatment which resulted in development of spherical CNCs where the high polydispersity of the spheres resulted in formation of a liquid crystalline phase.

A number of other researchers have reported the use of phosphoric acid in the hydrolysis process [34,35]. Camarero Espinosa *et al.* [34] optimized the hydrolysis process with phosphoric acid at 100°C with an acid concentration of 10.7 M for 90 min. The whiskers obtained under these conditions had an average length of 316 nm and diameter of 31 nm. A conductometric titration study showed a 10 times less surface phosphate groups compared to the sulfate groups after hydrolysis with sulfuric acid, indicating of very low charge density on the CNC surface. The thermal stability of the CNCs was studied with thermogravimetric analysis and compared with the CNCs obtained from sulfuric and hydrochloric acid hydrolysis. The results revealed that the phosphoric acid hydrolyzed CNCs had higher thermal

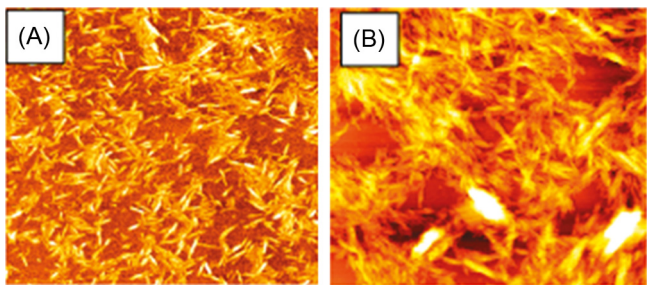

Figure 4.3 AFM images of cellulose nanocrystals obtained from (A) sulfuric acid and (B) hydrochloric acid hydrolysis of cotton.
Reproduced with permission from Ref. [31]. Copyright (2011) American Chemical Society.

stability compared to those bearing sulfate groups, but with less thermal stability compared to those obtained by hydrochloric acid process.

In another study [36], hydrobromic acid was used to prepare CNCs from cotton fibers. The optimization of the hydrolysis process was carried out by varying the reaction time, temperature, and acid concentration. It was found that the hydrolysis temperature of 100°C for 3 h of reaction with acid concentration of 2.5 M of HBr. Increasing the acid concentration from 1.5 to 2.5 M increased the yield. However, higher concentration of HBr was found to result in side reactions and produced darker nanocrystals. In addition, it was found that the application of ultrasonic energy especially at the intervals during the hydrolysis process enhanced the final yield of CNC extraction especially at lower reaction temperatures. This was attributed to the fact that the ultrasonic waves can break apart the microaggregates and provide higher surfaces for acid hydrolysis. In addition, at lower temperatures, the input from the ultrasound treatment can compensate for the lower thermal energy and significantly increase the overall yield.

4.2.2 Cellulose nanofibers from mechanical processes

A number of mechanical processes such as high-speed grinders [37], crushing in cryo-conditions [38], and high-pressure homogenizers [39] have been used to fabricate cellulose nanofibers from various starting source material. For example, Stelte *et al.* [39] studied the fibrillation process on soft and hard wood pulp to extract cellulose nanofibers. It was shown that the hard wood pulp needed more refining and high-pressure homogenization treatments by pressure-explosion technique to obtain nanofibers with similar properties. The nanofibrillation process is based on application of high shear force applied on the longitudinal axis of the cellulose fibrils, resulting in extraction of micro/nanofibrillar structures. In fact, additional repeated steps of high shear defibrillation result in relatively more uniform and smaller cellulosic fibrillar domains but with a compromise of less mechanical properties due to more damage impacted on the cellulose structure at each step.

It should, however, be noted that in order to extract the cellulose whiskers or nanocrystals, usually, a postchemical treatment is required to remove any remaining amorphous areas in the cellulose fibrils [40]. For example, Cherian *et al.* [41] developed cellulose whiskers from pineapple leaf fibers by a combination of high-pressure defibrillation and acid hydrolysis. They reported that by using repeated steps of acidic treatment using oxalic acid in autoclave with a high pressure resulted in effective defibrillation of banana fibers into nanoscale fiber with a length of about 200−250 nm and diameter of 4−5 nm.

4.2.3 Cellulose nanocrystals from ionic liquid process

ILs are molten salts that typically have melting points below 100°C due to their weak coordination of ions; and a number of them are liquid at or below ambient (room) temperature [42]. ILs have attracted considerable research attention over the past years in academia because they possess a large number of interesting physiochemical

properties like high electrical conductivity, chemical stability, nonflammability, near-zero vapor pressure, and tunable structure with a wide range of anions and cations [43]. Kilpeläinen *et al.* [44] showed that imidazolium-based ILs such as 1-butyl-3-methylimidazolium chloride are capable of dissolving cellulose under mild conditions and the regenerated cellulose from the IL solution shows various types of microstructure and morphologies. In one of the early studies, Li *et al.* [45] described a novel method based on using sulfuric acid hydrolysis process in 1-butyl-3-methylimidazolium chloride that significantly accelerated the reaction rate without any pretreatment. It was observed that in the course of the reaction, both endoglycosidic and exoglycosidic scission occurred, with the former being the dominant product in the initial stage of the reaction. The mechanism proposed by the authors for the accelerated reaction rate was ascribed to the dissolution of the cellulose in IL making the β-glucosidic bonds more accessible to the H^+ of the acid. In addition, the Cl^- from the dissociation reaction of the IL was thought to have a weakening effect on the glucosidic bonds thereby favoring the reaction under acidic conditions.

In a study by Man *et al.* [46], a novel approach based on using the 1-butyl-3-methylimidazolium hydrogen sulfate (bmim[HSO_4]) was used to prepare CNCs from microcrystalline cellulose (MCC). This preparation method was performed at a temperature range of 70−90°C for 1 h. The reported results indicated that the regenerated cellulose after treatment with IL maintained the same cellulose *I* structure with an increase in crystallinity index as the treatment temperature increased. It was also found that no cellulose derivative was formed upon treatment with IL and the length and diameter of the nanocrystals obtained from this method were, respectively, 50−300 and 14−22 nm and had less thermal stability compared to MCC. In a recent study, Tan *et al.* [47] used similar IL (bmim[HSO_4]) both as a solvent and reactant to extract CNCs from MCCs. They also observed that increasing the reaction temperature from 70 to 90°C resulted in enhanced crystallinity of the final CNCs. The main advantage of the IL-based techniques was the recovery of the IL after reaction ($>90\%$) with no harmful reaction byproducts.

In another interesting research reported by Abushammala *et al.* [48], CNCs were directly derived from wood particles using an acetate IL (i.e., [EMIM][OAc]) at 60°C with 2 h of reaction. A 20% by weight of the original wood mass was recovered in the form of CNCs with over 70% crystallinity in the form of cellulose *I*. The obtained CNCs were found to be partially acetylated from the solvation and reaction in the IL. The main mechanisms behind this process were reported to be (1) dissolution of lignin directly in the IL solution and swelling of the cellulosic portion, (2) decreased intermolecular hydrogen bonding via partial acetylation, and (3) catalysis of cellulose hydrolysis to produce the CNCs. In fact, the acetate IL ([EMIM][OAc]) had been shown previously to be able to dissolve lignin [49]; therefore, it is of great advantage to be able to remove the delignification process as a separate step in preparation of CNCs directly from wood particles. It is worthy to note that use of ILs is a promising approach to extracting CNCs from cellulose sources and the future studies be aimed at application of proper anion/cation pair in the IL and optimized reaction conditions to increase the CNC recovery yield with relatively higher aspect ratio whiskers.

4.3 Surface modification of cellulose nanocrystals: polymer/nanocellulose interfaces

Cellulose whiskers possess hydroxyl-rich surfaces with the potential of developing interconnected percolated network structure of hydrogen-bonded whiskers in polymer matrix with significant improvement of structural properties [50,51]. Note that this network structure may pose a challenge regarding both interfacial adhesion and efficient dispersion in relatively more hydrophobic polymer matrices [52,53]. This special surface property of the cellulose at nanoscale just mentioned, if controlled properly, can provide significant opportunities that can be exploited to engineer the surface in order to enhance the polymer/CNC interfacial adhesion and to improve CNC dispersion in the polymer to achieve optimal interfacial area with the host polymer. However, care should be taken to ensure that the morphology and structural properties of the CNCs are preserved during the surface modification reaction. The approaches that have been adopted so far to tailor the surface chemical functionality of CNCs can be categorized into three major routes: (1) generation of various chemical functionalities depending on the application using surface synthetic methods, (2) physical adsorption of surfactants/compatibilizers via physical forces such as electrostatic or hydrogen bonding, and (3) grafting of polymeric chains using both "graft onto" and "graft from" approaches. Some of the recent advances using these techniques are now described briefly as in the following sections.

4.3.1 TEMPO-mediated surface oxidation

TEMPO [(2,2,6,6-tetramethylpiperidine-1-oxyl) nitroxy radical]-mediated surface oxidation is based on using in combination with strong oxidizing agents such as sodium hypochlorite (NaOCl) that selectively oxidizes the surface methylol groups (primary alcohol) into carboxylic acid units [54,55]. A study by De Nooy *et al.* [56] showed that methylol groups are the only hydroxyls that can undergo the oxidation process while the secondary hydroxyl groups remain intact as they are deeply embedded within the whisker highly crystalline structure and, therefore, not accessible for the oxidation reaction. The carboxyl functional groups on the surface of cellulose can promote aqueous dispersion by electrostatic repulsion and provide colloidal stability. While the TEMPO-mediated oxidation has been shown to be easily tunable to control the extent of surface carboxylation by controlling the initial oxidizing agent content, excessive treatment is known to result in a decrease in the nanocrystal size due to the "peeling" reaction that removes the outer layer of cellulose from the crystal surface [57].

Li and *et al.* [54] developed nanocomposites of polyphenol via enzymatic polymerization in presence of TEMPO-oxidized nanocellulose. Their reported result revealed that due to the strong interfacial interaction between the polyphenol matrix and the surface carboxyl groups of the CNC, the thermal stability of the nanocomposite increased while the observation of the nanocomposite fractured surface indicated improved fracture toughness. The surface carboxyl groups can also be

utilized for further surface modification of the CNC to enhance the compatibility with the matrix. For example, Benkaddour *et al.* [58] developed a grafted polycaprolactone (PCL) on the cellulose whiskers that were previously oxidized by TEMPO. The authors demonstrated that the surface carboxyl groups were first esterified with 10-undecyn-1-ol, which was then subsequently utilized to undergo "click" chemistry with azide functionalized PCL that resulted in formation of surface PCL-*g*-CNC nanoparticles.

4.3.2 Silylation and acetylation of cellulose nanocrystal surfaces

The idea of sylilation of CNCs originated from the modification of cellulosic fibers with organosilane coupling agents that is a widely used method of surface functionalization of cellulose and wood fibers with prescribed functionality especially in polymer composite applications [59−61]. In this method, the surfaces of the CNCs are covered with crosslinked polysiloxane layers with desired functionality on the surface of the silane layer chosen to be compatible with the polymer matrix to enhance the interfacial adhesion. Typically, alkyl-dimethyl chlorosilanes are used and the surface chemistry involves evolution of HCl and formation of Si−O−C bond between the siloxane layer and CNC surface. Goussé *et al.* [62] studied the role of the alkyl chain length on the structure of partially silylated CNCs ranging from isopropyl to *n*-butyl, *n*-octyl, and *n*-dodecyl moieties. The surface of the CNCs was characterized based on degree of substitution (or DS) of the silane. It was found that a DS value of 0.6−1 preserved the whisker morphology of the CNCs. However, DS values higher than 1 resulted in deformation and loss of the original whisker morphology. In addition, the partially silylated whiskers were found to be readily dispersible in organic solvents such as THF. In order to reduce the surface hydrophilicity and make the CNCs compatible with cellulose butyrate acetate matrix, Grunert *et al.* [21] carried out trimehtylsilylation of the CNC surface in formamide. Yu *et al.* [63] used 3-isocyanatopropyltriethoxy silane via the reaction of isocyanate groups of the silane coupling agents with CNC surface hydroxyls catalyzed by $Sn(Oct)_2$ in anhydrous Dimethyl Formamide (DMF) and incorporated the modified CNCs in silicon elastomer. These surface modifications gave better dispersion of CNCs in the respective polymer matrices and significant improvement of mechanical properties of the final nanocomposite elastomers. In an alternative method, Raquez *et al.* [64] used an aqueous solution of methacryloxypropyltrimethoxysilane in a suspension of cellulose whiskers followed by the hydrolysis of the silane. The observed modified CNCs were recovered through centrifugation and vacuum drying or freeze−drying after the adsorption step. The condensation of silane on CNC surface was achieved by curing the silane-adsorbed-CNC particles in a vacuum oven at 110°C. In addition, the authors showed that application of an excessive amount of silane (more than 200 mM) was not attainable due to the formation of a biphasic solution. This method was called a "green and sustainable" approach because it eliminates the evolution of HCl as in the case of chlorosilane agents.

Surface acetylation of CNCs has mostly been achieved through utilization of various anhydride-based compounds. Yu *et al.* [65] prepared acetylated CNCs by

reacting succinic anhydride with CNCs under pyridine reflux and the unreacted anhydride was removed by successive washing with water, acetone, and ethanol. These carboxylated CNCs were used for metal ion adsorption applications. In another simple approach [66], alkenyl succinic anhydride aqueous emulsion was mixed with CNC suspension and freeze-dried followed by heating at 105°C to produce highly hydrophobic CNC particles that were dispersible in low polarity solvents such as 1,4-dioxane. Sassi *et al.* [67] studied the role of the reaction medium on structure of CNCs during acetylation reaction. Using a nonswelling reaction mechanism where only surface cellulose chains are considered, they found that when acetylation is carried out under homogenous reaction conditions, the acetylated layers of the whisker are immediately released in the reaction medium after obtaining sufficient solubility. However, under heterogeneous reaction conditions, only surface cellulose chains are acetylated, resulting in formation of a layer of nonsoluble cellulose acetate that surrounds the highly crystalline core of unreacted cellulose.

4.3.3 Polymer grafting by surface-initiated polymerization

Ring-opening polymerization (ROP) has been one of the major routes to grafting polymer chains from the surface of cellulose substrates due to the presence of surface hydroxyl groups that can act as polymerization initiation sites [68]. In an early study, Hafrén *et al.* [69] used surface-initiated ROP to graft PCL onto cotton and filter paper surface where the reaction was catalyzed by organic and amino acids. Habibi *et al.* [20] used the same concept to graft PCL through surface-initiated ROP catalyzed by $Sn(Oct)_2$ from the CNC surface. Their results suggested that the structure and morphology of the CNCs remained intact after the grafting reaction. The obtained modified CNC particles showed significantly improved dispersion and compatibility with a PCL matrix in a nanocomposite material. Carlsson *et al.* [70] studied the effect of ROP reaction time on surface properties and grafting density of the PCL on the CNC surface characteristics. Their results showed that the surface graft density was constant at 3%−7% and independent on the ROP reaction time. In order to enhance the efficiency of the reaction, Lin *et al.* [71] used microwave-assisted surface-initiated ROP to graft PCL on CNC surface. The obtained modified CNC was melt mixed with PLA matrix to give a nanocomposite that showed enhanced interfacial compatibility with the hydrophobic matrix. In another approach to prepare hydrophobically modified CNCs, Morandi *et al.* [72] grafted polystyrene chains onto CNC surface via surface-initiated atom transfer radical polymerization (ATRP). This approach used a 2-bromoisobutyryl bromide as the ATRP initiating site on the CNC surface followed by polymerization. The brush chain length and grafting density were easily controlled by adjusting the reaction conditions. Using a similar approach, Zeinali *et al.* [73] prepared thermoresponsive CNC whiskers by grafting poly(*N*-isopropyl acrylamide) and pol(acrylic acid) through surface-initiated reversible-addition fragmentation transfer polymerization by attaching 2-(dodecylthiocarbonothioylthio)-2-methylpropionic acid as chain transfer agent followed by polymerization of acrylic monomers.

4.3.4 Cellulose surface modification by electrostatic and physical adsorption

This approach toward modification of CNC surface is based on utilization of physical forces such as electrostatic attraction or hydrogen bonding to adsorb various functional molecules or polymers on the CNC surface especially when the CNC is prepared by sulfuric acid hydrolysis that leaves the surface negatively charged. Application of surfactants has been shown to be a promising method of interfacial compatibilization of cellulosic fibers with polymer matrix [74,75] where the hydrophilic head of the surfactant interacts with the hydrophilic surface of cellulose, and the hydrophobic tail interacts with the matrix. For example, Hu *et al.* [76] used surfactants such as didecyldimethylammonium bromide and cetyltrimethylammonium bromide to modify the surface of CNC through electrostatic attraction of positively charged surfactant and negatively charged CNC surface. They found that the morphology of the surface layer on CNC surface was concentration dependent where low concentrations resulted in brush-like morphology with hydrophobic tails of the surfactant pointing outward thereby rendering the CNC surface highly hydrophobic. On the other hand, higher concentrations resulted in aggregation of surfactant on the CNC surface with a decrease in hydrophobic character. Salajková *et al.* [77] modified the surface of the TEMPO-oxidized nanocellulose with various functional groups such as epoxide, benzyl, and acrylate groups through the use of the corresponding ammonium salt adsorbed on the surface through electrostatic force. This was demonstrated to be a promising method for composite applications because various chemical functionalities can be introduced on the CNC surface that, in turn, could potentially interact/react with the host matrix polymer. The use of nonionic surfactants such as sorbitan menstruate has also been used to disperse CNCs in hydrophobic matrix [78,79]. Another approach for modification of CNC surface is based on layer-by-layer (LbL) adsorption as described in the next section. In summary, a schematic representation of various CNC surface modification techniques is shown in Fig. 4.4 for clarity and easy access.

4.4 Processing and development of CNC-based hybrid polymer nanocomposites

In this section, a brief overview is given of the most commonly used approaches in preparation of thermoplastic and thermoset polymer nanocomposites based on CNCs.

4.4.1 Solvent casting

Solvent casting is the most widely used technique for preparing CNC-based nanocomposites [80]. In a typical process, the CNCs are dispersed in the dispersing medium which is mostly aqueous dispersions although other solvents have been used. Once fully dispersed, the polymer is added to the dispersion, and the final

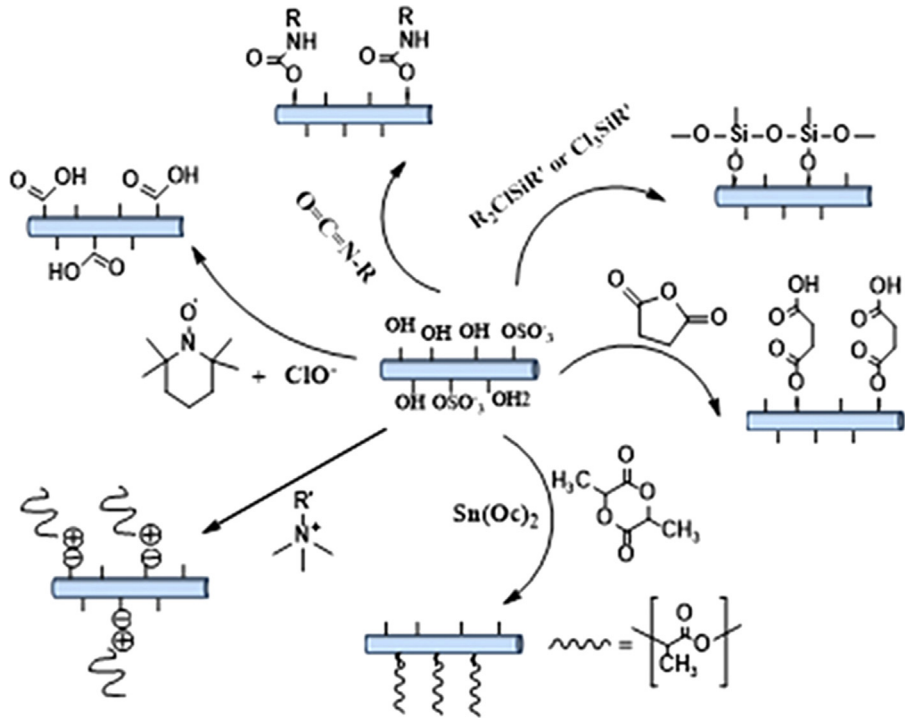

Figure 4.4 Common surface modification chemistries of cellulose nanocrystals.

nanocomposite hybrid material is developed by removing the solvent. Aqueous dispersion is a highly favorable dispersion medium because the CNCs can be readily dispersed in water at nanoscale without aggregation. However, one limitation of this technique is the fact that only water-soluble/dispersible polymers or latex materials can be formulated. Paralikar *et al.* [81] prepared nanocomposite membranes of CNC incorporated into polyvinyl alcohol (PVOH) through solvent casting in water. The membranes had CNC concentration of 0−20 wt%. The process involved mixing of two separate master batches of a solution of PVOH and dispersion of CNC in water followed by a sonication of 25 min for breaking up any agglomerates formed during mixing. Because of the high solubility of PVOH and dispersibility of CNC in water, a synergistic effect of the CNC/PVOH interaction was observed as evidenced by highly dispersed CNCs in the PVOH membrane that resulted in enhanced physical and mechanical properties. Azizi Samir *et al.* [82] used water-based casting technique to prepare poly(oxyethylene) (POE) nanocomposite reinforced with CNCs. In their method, CNCs were dispersed in the POE solution and mixed for 24 h followed by drying at 40°C for a week and at 100°C for 72 h.

In addition to water, a number of polar organic solvents have also been successfully used as dispersing medium for preparation of CNC-based nanocomposites such as DMF [83], dimethyl sulfoxide (DMSO), and *N*-methyl 2-pyrrolidone (NMP) [84].

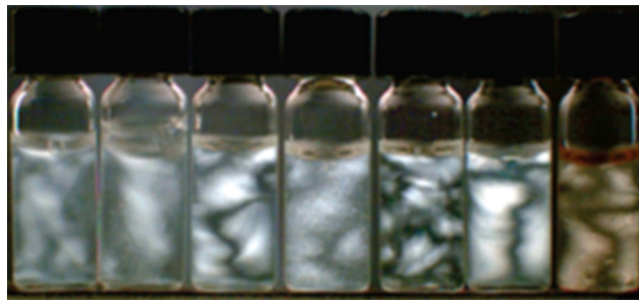

Figure 4.5 Dispersion of sulfuric acid hydrolyzed CNC through cross polarizers from left to right: as prepared in water, freeze-dried, and dispersed in water, DMF, DMSO, NMR, formic acid, and *m*-cresol.
Reproduced with permission from Ref. [84]. Copyright (2007) American Chemical Society.

In a recent study by Van den Berg *et al.* [84], the dispersibility of the cellulose whiskers in various organic solvents based on the surface charge of the whiskers was studied. It was found that the presence of negative surface charges (sulfate groups) obtained from sulfuric acid hydrolysis as already described is necessary for successful dispersion of whiskers in polar solvents such as DMSO, DMF, and NMP as shown in Fig. 4.5. However, protic solvents such as the formic acid and *m*-cresol are able to disperse even the CNC whiskers with neutral surfaces due to their ability to disrupt the intraparticle hydrogen-bonded network structure.

Marcovich *et al.* [85] used DMF as suspending agent to obtain a stable suspension of CNCs using ultrasonic treatment. This stable suspension was then added to a mixture of polyol-isocyanate to obtain CNC reinforced polyurethane films. Using a similar approach, Liu *et al.* [86] fabricated PMMA nanocomposite reinforced with up to 10 wt% CNCs. This facile preparation method involves mixing of a stable suspension of CNCs in DMF with a solution of hydrophobic PMMA in DMF and drying the resulting mixture to give cast solid composite films with enhanced benefits.

Solvent exchange process is another method of transferring cellulose whisker dispersions to organic solvents from aqueous dispersion. The advantage of this technique is the fact that a percolating network structure of CNC whiskers can be obtained in the aqueous solutions that can be directly transferred to organic solvent in the form of "organo-gels." This method is known as the template approach developed by Capadona *et al.* [87,88]. In this method, a dispersion of CNC in water is solvent exchanged with acetone over a period of a week through formation of aqueous−organic bilayer mixture. The solvent exchange results in development of an organo-gel of CNCs in acetone. Nanocomposites of ethylene-oxide/epichlorohydrin copolymer were prepared by the template approach by placing the CNC-in-acetone organo-gel in the copolymer solution followed by compression molding and drying. The obtained nanocomposites developed by this novel approach had mechanical properties comparable with that of samples that were directly solution-cast in DMF. Wang *et al.* [89] used the same organo-gel template approach to prepare poly(propylene-carbonate) green nanocomposites reinforced with CNCs. The reported morphological observations showed a submicron scale dispersion of

the CNCs within the matrix polymer which was further confirmed by enhancement of mechanical properties. The solvent exchange process has also been used to transfer CNCs from aqueous solutions to highly water-immiscible solvents such as toluene [90] in order to prepare atactic PP/CNC nanocomposites. By contrast, severe aggregation of CNCs was observed in toluene.

Other approaches such as surface modification of CNCs with more hydrophobic functionalities [91] or long chain hydrophobic moieties [92] have also been used in order to disperse the CNCs in water-immiscible solvents. Note, however, that although a good dispersion of particles may be achieved, the interaction of particles through hydrogen bonding and formation of interconnected network structure would be severely limited.

4.4.2 Melt processing

Although solvent casting process is effective in achieving fine dispersion of CNCs in polymer matrices that is a necessary requirement of effective property enhancement of the host polymer matrix, it is both lengthy and noneconomical approach from the practical application point of view because the plastic industry is more interested in solvent-free "green" processing methods with significantly shorter cycle times. In this context, melt extrusion is the most widely used polymer processing technique in industry for fabrication of composites and nanocomposites [93]. However, there is a challenge of obtaining a well-dispersed morphology of CNC in the polymer matrix during extrusion because CNC tends to severely aggregate when blended with hydrophobic thermoplastics. A significant number of studies have been reported in the literature for the preparation of polymer/CNC nanocomposites using extrusion process such as polyethylene [94,95], polypropylene [96,97], polystyrene [98], polylactic acid [99,100], polyvinyl chloride [101] and poly(3-hydroxybutyrate-*co*-3-hydroxyvalerate) (PHBV) [102], PCL [103], and thermoplastic starch [104]. Typically, a surface modifier such as a graft polymer layer or surfactant or simply a compatibilizer is used in order to enhance the CNC dispersion and compatibility with the matrix. For example, Bondeson *et al.* [105] prepared a suspension of the cellulose whiskers with PVOH and introduced the mixture in the PLA matrix with extrusion process using dry and liquid feeding techniques. It was found that although liquid feeding produced a better dispersed morphology of the CNCs in the PLA, the majority of the particles were located inside a discontinuous phase of PVOH within the continuous PLA matrix phase. Direct pumping of an aqueous solution of CNCs into the PLA matrix in the extrusion process did not show any improvement in the structural properties of the nanocomposites due to poor dispersion of CNCs in the matrix [106].

Application of 5 wt% anionic surfactant [99] was found to improve the dispersion of CNCs in the PLA matrix during extrusion with improved mechanical properties. However, higher surfactant content was found to degrade the PLA matrix. In another approach, Goffin *et al.* [107] grafted PLA chains on the CNC surface via surface-initiated ROP and melt extruded the modified CNC particles with PLA matrix. The results showed enhanced compatibility between the obtained PLA-*g*-CNC and PLA matrix indicated by improvement of mechanical properties and promotion of crystallization nucleation in the matrix. A similar strategy [20] was used to graft PCL

on the CNC surface by ROP and reported that gave significantly improved dispersion as a consequence of the PCL graft layer due to enhanced interfacial compatibility.

In the case of polyethylene matrix, de Menezes *et al.* [94] grafted fatty acid chains on the CNC surface and melt extruded the modified particles with low-density polyethylene matrix. The results showed that increasing the fatty acid chain length enhanced the dispersion of the CNCs in the LDPE matrix. Ben Azouz *et al.* [95] prepared a dispersion of CNCs in high molecular weight polyethylene oxide (PEO) solution to wrap the CNC surface with PEO layers. Subsequently, they freeze-dried the mixture and used in the desired product in an extrusion process to incorporate the modified CNCs in the Polyethylene (PE) matrix. As shown in Fig. 4.6, the extrusion of PEO-modified CNC with PE resulted in no significant degradation of particles while direct melt mixing of CNC with PE resulted in severe discoloration. This is thought to be a promising approach in order to effectively disperse the CNCs in the hydrophobic matrix while preserving their thermal stability during melt processing. Interestingly, similar approach [102] used polyethylene glycol (PEG) instead as the surface wrapping agent for CNCs in PHBV matrix during the high shear extrusion process, and the obtained results showed that the PEG layer was completely removed from the CNC surface and mixed with the PHBV matrix, leaving the cellulose whiskers aggregated in the matrix. Consequently, therefore, the molecular weight of the wrapping agent was found to be the determining success factor in this method.

4.4.3 In-situ polymerization

In-situ polymerization is a versatile approach in the preparation of nanocomposite materials with possibilities of obtaining highly desirable morphologies and tunable

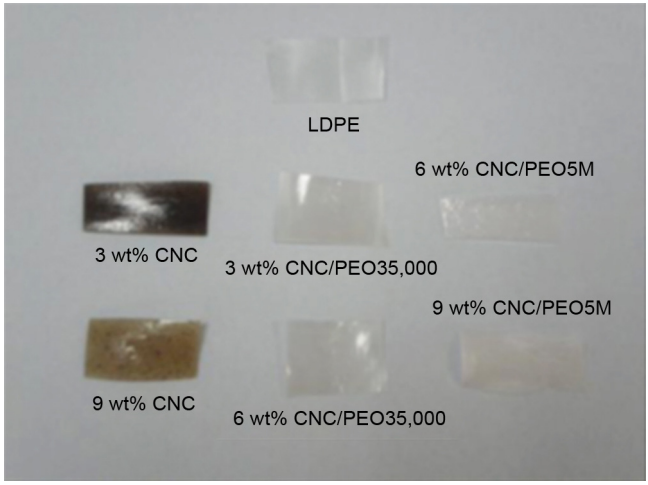

Figure 4.6 Melt extruded PE nanocomposite reinforced with unmodified and PEO-modified CNC and the subsequent color change during processing.
Reproduced with permission from Ref. [95]. Copyright (2011) American Chemical Society.

functionalities of hybrid materials [108]. In this method, the nanoparticles are dispersed or mixed with the monomer (in liquid form) followed by polymerization of monomer in presence of nanoparticles through various polymerization mechanisms [108]. In the case of CNC nanocomposites, this approach has been utilized for both thermoset and thermoplastic matrix materials. Liu *et al.* [109] prepared phenolic thermoset polymers reinforced with cellulose whiskers. Phenol-formaldehyde (PF) resin was first mixed with an aqueous dispersion of CNC which as then solvent exchanged with DMF through three successive cycles. The solution was then treated with a stepwise curing profile to obtain fully cured PF/CNC nanocomposite films. Tang *et al*. [110] prepared epoxy-based nanocomposites reinforced with cellulose whiskers. The preparation involved mixing a dispersion of CNCs in DMF with DGEBA monomer and toluenediamine-based curing agent followed by casting and curing. No phase separation occurred during curing and the CNC whiskers were found to be evenly dispersed within the epoxy matrix.

Polyurethane-based nanocomposites with CNCs have also been prepared with in-situ polymerization approach [14,111–113]. Li *et al*. [111] prepared PU nanocomposite foams with CNCs using sucrose-based polyol, a polymeric diphenylmethane diisocyanate, and a glycerol-based polyol. Upon polymerization, development of extra hydrogen bonds and additional crosslinks between the PU and hydroxyl groups of the CNC surface was confirmed, resulting in significant enhancement of properties at low CNC volume fractions. Strong reinforcement effect of CNCs was observed in elastomeric PU nanocomposites [112] which was attributed to the increasing number of crosslink density due to the interfacial bond formation between the CNC surface and PU hard-microphase domains.

Furfuryl alcohol (FA) has been in-situ polymerized in presence of cellulose whiskers [114,115] to fabricate fully bio-based nanocomposite materials where the FA acted both as the dispersant of the CNC as well as the polymerization precursor. It was found that the residual sulfonic acid groups on the surface of hydrolyzed cellulose whiskers catalyze the ROP of FA.

In our previously reported study [116], we demonstrated the development of polyamide 6 nanocomposites reinforced with CNCs via in-situ ROP of ε-caprolactam. Nanocomposites containing up to 2 wt% of CNC in PA6 were prepared and found that the increasing the CNC content resulted in less monomer conversion due to anionic polymerization inhibition effect of the CNC particles. Analysis of the properties and morphology of the PA6/CNC nanocomposites revealed the formation of an interconnected CNC fibrillar structure that significantly changed the rheological behavior of the PA6 matrix and the creep resistance of the matrix was significantly increased.

4.4.4 Layer-by-layer assembly

LbL assembly has been shown to be a promising method of fabrication of nanocomposite thin films especially in biomedical application where high loading of nanoparticles such as carbon nanotubes in thin films has been achieved [117–119]. One of the early reports of preparation of composite thin films by LbL method was by Podsiadlo *et al.* [117] who successfully prepared a multilayered structure of

negatively charged sulfated CNCs with a poly-(dimethyldiallylamonium chloride) (PDDA) polycation on a glass substrate through multistep dipping in CNC and PDDA solutions. Mesquita *et al.* [120] developed bio-based highly deacetylated chitosan−CNC multilayered composite films through LbL assembly. The driving force for development of the layered film is reported to be the electrostatic attraction between the negative surface charge of CNC and positive charge of chitosan as well as the strong hydrogen bonding among layers. Morphological observations on the samples revealed a 7-nm thickness for each bilayer. In another study [121], high aspect ratio CNCs were assembled into "flattened matchstick pile" structures for antireflective coating applications. At optimum assembly conditions, the authors reported a 100% light transmittance through the film.

Thin films of polyelectrolyte/CNC nanocomposites [122] were prepared using solution-dipping and spin-casting methods with improved optical properties. It was reported that the spin-coated films were much thicker than the films prepared by solution-dipping method. In addition, the former system showed thin film interference colors and optical properties that were easily tunable through processing method. In addition to the reported studies on development of bio-based thin film composites by LbL assembly approach with superior gas barrier properties [123,124], it is worthy to note that these novel thin films have great potential, when combined with biodegradable and biocompatible polymers such as collagen [125], to be applied as extracellular matrix with significant potential in biomedical applications.

4.5 Properties of polymer/cellulose nanocrystals nanocomposites

4.5.1 Mechanical properties

CNCs are attractive potential reinforcing additives for polymer matrices due to their exceptionally high mechanical properties and relatively lower density compared to most conventional nanoreinforcing agents that translates into nanocomposites with relatively lighter weight [126]. This is evidenced by considering the longitudinal modulus of CNCs to be in the range of 100−170 GPa with an average value of 130 GPa which is almost equivalent to that of aramid fibers [3]. Depending on the source of CNC extraction, various longitudinal modulus values have been reported (e.g., 105 GPa for the CNCs from cotton and 143 GPA for CNCs from tunicate) [127,128]. Transverse elastic moduli of cellulose whiskers were investigated by Lahiji *et al.* [129] at 30% and 0.1% relative humidity by Atomic Force Microscopy (AFM). They measured a transverse elastic modulus (E_T) value of 18−50 GPa for wood-derived CNC whiskers and the effective stiffness in higher relative humidity condition was found to be slightly higher. Wagner *et al.* [130] used AFM force−displacement measurements to estimate the transverse modulus of CNC whiskers derived from tunicate and found to range from 2 to 37 GPa. This large variation in measurement of ET by AFM was attributed to the uncertainties related with the sensitivity of AFM tip rather than the property variation.

Cao *et al*. [131] reported a significant mechanical property enhancement by CNCs in thermoplastic starch with tensile strength increasing from 3.9 to 11.5 MPa and elastic modulus increasing from 31.9 to 823.9 MPa, respectively, with increasing CNC content up to 30 wt%. In a study [132] on electro-spun PLA mats, addition of up to 5 wt% of CNCs resulted in 5- and 22-fold increase in tensile strength and modulus compared to that of neat PLA fiber mats, respectively. Biodegradable poly (butylene succinate) (PBS) foams reinforced by CNCs was developed by Lin *et al*. [133] and incorporation of 5 wt% of CNC in the foam resulted in 50% and 62.9% improvement in flexural strength and modulus, respectively, compared to neat PBS foams. The reinforcing capability of the CNCs has been demonstrated in a number of other studies on thermoplastic polymers such as PVA [134], PLA [135], PMMA [136], poly(vinylidene-fluoride) [137], poly(3-hydroxybutyrate) [138]. Engineering thermoplastics such as polyamide 6 have also been reinforced with CNCs [139,140].

In addition, CNCs have been used to mechanically reinforce elastomeric polymers as well. Biocompatible waterborne polyurethane matrix was reinforced with small volume fraction of CNCs (1 wt%) that increased the tensile strength and Young's modulus from 5.43 to 12.22 MPa and from 1.16 to 4.83 MPa, respectively [141]. The reinforcing efficiency of CNCs has also been demonstrated in natural rubber nanocomposites [142]. However, the addition of CNCs has been shown to decrease the elongation at break in the nanocomposite material compared to the host polymer matrix due to the stiffening effect of CNCs in the polymer [20,90]. Furthermore, the mechanical property enhancement has also been studied in thermoset polymers. Pan *et al.* [143] studied the reinforcing ability of cellulose nanocrystals in an epoxy-acrylate UV-curable transparent film. The DMA results indicated a significant enhancement of modulus above the glass transition temperature (i.e., rubbery state) with increasing CNC loading. The reinforcing effect of CNCs in a phenolic thermoset resin [109] was adequately described by Halpin−Kardos model suggesting the domination of matrix−filler interaction over filler−filler interaction. The studies of the effects of CNC on mechanical properties of unsaturated polyester resin were studied [144] where it was found that surface modification of CNC with organosilane coupling agents resulted in improvement of strength and stiffness of the of the polyester resin whereas no significant changes were observed on the impact energy of the polyester nanocomposites after the surface treatment.

There are a number of important characteristics of the cellulose whiskers that play a critical role in its mechanical reinforcement efficiency in polymer composites. Cellulose whiskers, owing to their nanoscale dimensions, have significantly large specific surface area which has been reported to be in the range of 100 $m^2\,g^{-1}$ to several hundreds $m^2\,g^{-1}$ [145,146]. This large available surface could in fact be exploited to enhance the interfacial interaction in CNC/polymer nanocomposites through favorable interfacial interactions such as hydrogen bonding [147]. Moreover, the available surface interfacial area between the CNC whiskers and the host polymer is governed by the state of dispersion of CNCs in the matrix as well as the effect aspect ratio of the whiskers. Good CNC dispersion in the polymer at the molecular level and its relatively large aspect ratio (i.e., ratio of length to diameter) will increase the interfacial area between the particles and the polymer.

The increased interfacial area will facilitate the stress transfer under mechanical load from the neighboring polymer chains to relatively very stiff and strong whiskers [148,149]. On the other hand, the highly hydrophilic nature of CNCs may lead to severe aggregation of whiskers in the polymer matrix which, in turn, reduces the available surface area, the effective aspect ratio, and the reinforcing potential of the whiskers. Rusli *et al.* [31] studied the role of CNC surface charge and aspect ratio and the corresponding microstructural properties on stress transfer efficiency from matrix to whiskers in an epoxy matrix by Raman spectroscopy. Their results demonstrated that the tunicate-derived cellulose whiskers had significantly higher stress transfer capability due to their exceptionally large aspect ratios compared to that of the cotton-derived whiskers. In addition, the sulfuric acid hydrolyzed samples had better dispersion throughout the matrix while the hydrochloric acid hydrolyzed whiskers showed negligible stress transfer capacity due to their excessive aggregation as a result of surface neutrality that, in turn, reduced their effective aspect ratio in aggregated state. In addition, the effect of interfacial compatibility between the matrix and CNC particles on mechanical properties was demonstrated by Goffin *et al.* [103] who used unmodified and PLA-*g*-CNC particles (by surface-initiated ROP of lactide) to reinforce PLA matrix. The reinforcing efficiency of the interfacial compatibility was shown by enhanced stiffness of the matrix above the *Tg* in the case of grafted CNCs.

The strong mechanical reinforcing ability of cellulose whiskers has spurred a number of researchers to use micromechanical models to theoretically describe the mechanical properties of polymer/CNC nanocomposites. However, it was found that the use of conventional short fiber composites models such as Halpin−Tsai equations failed in a number of polymer/CNC nanocomposites systems reported in the literature by underestimating the reinforcing ability of CNCs [150]. This was attributed to the formation of a percolating rigid network structure of CNC whiskers that are strongly bonded together through hydrogen bonding that is not accounted for in the theoretical equations. To better understand the mechanical reinforcing property of the CNC/polymer nanocomposites with a percolated structure, the series-parallel model of Takayanagi *et al.* [151] (as modified by Ouali *et al.* [152]) can be applied to predict the elastic shear modulus of the composite according to the following equation:

$$G_c^{'} = \frac{(1-2\psi+\psi\chi_r)G^{'}{}_rG^{'}{}_s + (1-\chi_r)\psi G_r^{'}2}{(\chi_r-\psi)G^{'}{}_s + (1-\chi_r)G^{'}{}_r} \tag{4.1}$$

where the subscripts r and s refer to rigid (whisker) and soft (polymer) phases and ψ is related with the volume fraction of the percolating phase (in this case the whiskers). The ψ parameter can be obtained using the following equations:

$$\psi = 0 \quad \text{for} \quad \chi_r < \chi_c \tag{4.2}$$

$$\psi = \chi_r\left(\frac{\chi_r-\chi_c}{1-\chi_c}\right)^b \quad \text{for} \quad \chi_r < \chi_c \tag{4.3}$$

In these equations, $b = 0.4$ for a three-dimensional percolating network, χ_c is the critical volume fraction at which the percolation begins. According to Favier *et al.* [50], this parameter can be estimated using the equation $\chi_c = 0.7d/l$, where d and l are the diameter and length of the whiskers. χ_r is the volume fraction of the rigid whiskers phase. At sufficiently high temperatures, the stiffness of the matrix can be assumed to be zero and the equation is then simplified to $G'_c = \psi G'_r$.

It has also been explained that the good agreement between the experimental data and the values predicted by the model just described that takes the percolating phase structure into account is ascribed to the formation of infinite agglomerations of cellulose whiskers. It is also worth noting that the percolation threshold and structure formation of CNC network structure in the matrix can be controlled by the interfacial interaction, compatibility with the matrix the dispersion quality, and the original aspect ratio of the fibers. The larger the effective in-situ aspect ratio of the CNCs in the matrix, the lower the volume fraction at which a percolating network structure of the CNCs is formed.

4.5.2 Thermal properties

The thermal properties of CNC/polymer nanocomposites such as the thermal stability, glass transition temperature, melting, and crystallization behavior are important variables in development of the novel functional nanocomposites. Roman *et al.* [153] studied the effect of sulfate groups on the CNC surface on the thermal stability of sulfuric acid hydrolyzed bacterial cellulose whiskers through controlling the sulfuric acid hydrolysis conditions. They reported a significant decrease in thermal stability of the CNC as the sulfate groups increased on the surface. It was also reported that the sulfate groups increase the char fraction after thermal degradation, implying the additional role of the CNCs as flame retardants. Note that the presence of sulfate groups catalyzed the degradation processes as indicated by relatively lower thermal degradation activation energy in CNCs with high sulfate group's concentrations. Similar observations were made with thermal stability of the CNCs prepared by enzymatic process which was found to be higher than those of sulfuric acid hydrolyzed [10]. Incorporation of bacterial grown CNCs into PVA matrix resulted in significant thermal stability improvement from the onset temperature of thermal degradation of 184°C in the case of sulfuric acid hydrolyzed CNC in PVA to 378°C in the case of the bacterial grown CNC in PVA matrix. The presence of CNCs in a PMMA matrix [86], however, showed only slight reduction in the onset temperature of thermal degradation with the addition of CNCs. It is clear that a strong interfacial interaction or chemical bond facilitates enhancement of thermal stability in CNC-based nanocomposite. In such cases, the presence of CNC in the matrix is advantageous for thermal stability of the host polymer matrix by increasing the energy required for the onset of polymer decomposition and associated reduction in thermal expansion [154,155].

Considering the effect of CNCs on the glass transition temperature of host polymers, a great number of studies have reported no obvious change in systems including but not limited to poly(styrene-*co*-butyl acrylate) [156], PVC [157], PP [90],

POE [82], and natural rubber [158] nanocomposites. On other hand, polymers that form strong interfacial interaction with the CNC surface through hydrogen bonding have typically increased *Tg* with incorporation of CNCs. For example, in our previously reported study [116], we demonstrated that the *Tg* of the amorphous portion of polyamide 6 increased slightly with a small volume fraction of CNCs. In addition, a similar effect has been observed in strong hydrogen bond-forming matrices such as PVOH [10] and glycerol plasticized starch [159] where the strong interfacial interaction severely inhibits the molecular motion and viscous flow of the polymer chains, resulting in an increasing trend of glass transition temperature with addition of CNCs.

The melting temperature of semicrystalline polymers has also been affected by CNCs in various ways to an extent that depends on the surface chemistry and interfacial interaction of polymer with CNC surface. For example, in a number of systems such as poly(ethylene oxide) [82], cellulose acetate butyrate [21], plasticized starch [160], and PCL-based nanocomposite [161], no significant change in melting behavior of the polymer was observed. However, surface-modified CNCs have been shown to promote the crystallization of some particular polymer systems. For example, in the cellulose acetate butyrate system, trimethylsilylation of CNC surface resulted in enhanced crystallization and increased melting temperature of the matrix that was attributed to the promotion of polymer−CNC interfacial interaction by surface modification. In another study [113], a completely amorphous polyurethane elastomer was found to transform into a thermoplastic-like material with partial crystallinity when CNCs with a surface layer of grafted polyurethane prepolymer were incorporated in the matrix.

Crystallization behavior of the CNC nanocomposites is also affected by the presence of the CNCs depending on their surface chemistry, dispersion quality, and microstructure development within the host polymer matrix. Pei *et al.* [162] studied the role of surface modification of CNCs with silane agent on crystallization behavior of PLA and found that the modified CNC particles were very well dispersed in the PLA matrix and enhanced the crystallization kinetics by acting as effective nucleating agents. However, no such effect was found for nonmodified CNCs because they formed highly aggregated structures in the matrix. Gray *et al.* [163] reported strong nucleating effect of CNC in PP matrix as evidenced by the development of a transcrystalline layer on the cellulose surface as shown in Fig. 4.7. Han *et al.* [164] studied the role of cellulose whiskers in polyurethane matrix during isothermal crystallization by using Avrami model and found that the CNCs act as nucleating agents during isothermal crystallization.

4.5.3 Melt rheological properties

Rheology is a powerful tool to study the effect of nanoparticle additives and their interaction with matrix on viscoelastic and microstructural properties of the nanocomposites. In addition, rheological data provide helpful insights into the behavior of the nanocomposite and hybrid materials during the melt processing stage. As in the case of nanoparticulate-filled polymer composites, rheological properties can provide fundamental understanding of the structure−property relationships in

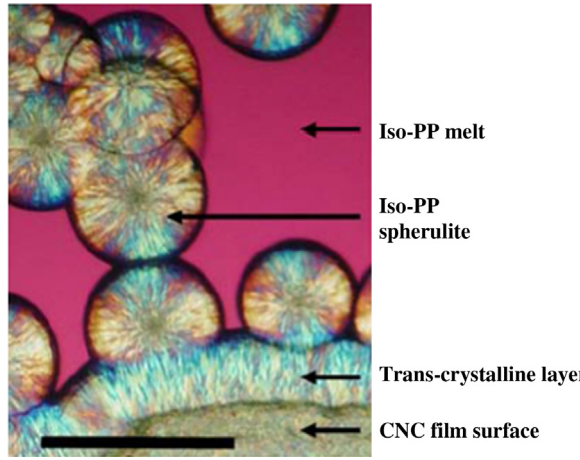

Figure 4.7 Development of transcrystalline layer iso-PP crystal on the CNC film surface. Reproduced from Ref. [163] with permission from Springer.

CNC-based nanocomposite materials. Typically, this is accomplished through observation of changes in viscoelastic variables such as the storage and loss modulus (G' and G''), complex viscosity (η^*), and tan δ. In a series of studies on rheological behavior of CNC suspensions [165−167], it was observed that the suspension develops strong elasticity at high concentrations where the behavior resembles that of an elastic gel. Temperature sweep experiments indicated a structural rearrangement between 30°C and 40°C, where G' initially increases and then decreases at higher temperatures. The structure formation was also confirmed in a sonicated CNC suspension by observation of the failure of Cox−Merz rule [168]. Rheological analysis of nanocomposites of PHBV reinforced with CNCs [169] revealed that the most rapid changes in the G' and G'' occurred in the concentration range of 0.5−2 wt% of CNC while the viscoelastic transition crossover point occurred at 1.2 wt% of CNC above which the nanocomposite melt behaved like an elastic gel. In our previously reported study [116] on polyamide 6 nanocomposites, we demonstrated the formation of CNC network structure within the PA6 matrix. It was shown that the formed structure could be broken apart by application of 10 s^{-1} shear rate and reformed upon removal of shear. In fact, the failure of the Cox−Merz rule for the samples with the highest concentration of CNC studied (i.e., 2 wt%) confirmed the structure formation. Increasing the CNC concentration from 0.6 to 2 wt% was also associated with a decrease in the slope of the terminal zone of the plot of G' and G'' versus frequency that was attributed to enhanced elasticity of the melt upon increasing the CNC concentration. In a study on polyurethane nanocomposites reinforced with CNCs [85], the onset of percolation was found to be 1 wt% of the CNC. Above this concentration, a network of H-bonded whiskers formed throughout the matrix. This network was easily destructible by shear in the nonlinear viscoelastic zone. Mahi *et al.* [170] studied

the linear and nonlinear rheological properties of ethylene vinyl acetate copolymer nanocomposite reinforced with CNCs. Small amplitude oscillatory shear experiments showed a significant enhancement of melt elasticity as shown in Fig. 4.8A and B by development of a nonterminal behavior in storage and loss modulus versus frequency which is indicative of transition to pseudosolid like behavior. The onset of percolation and network formation significantly affects the long-range motion of polymer chains in the low-frequency region and prevents the polymer relaxation as in the case of the neat polymer melt. The transient shear experiments did not show an overshoot in low shear region while an overshoot developed at high shear rates. This observation was attributed to the nanonetwork break up and orientation in the flow direction as schematically depicted in Fig. 4.8C and D.

A similar increase of storage and loss modulus was also observed in various CNC-based nanocomposite systems such as polyurethane [171], poly(ethylene-glycol) [172], nitrile rubber [173], POE [95], and poly(vinyl acetate) [174].

The complex viscosity (η^*) of the nanocomposites is also affected by the presence of nanocrystals in the polymer melt. Normally, addition of stiff rigid nanoparticles with high surface area results in increase of the complex viscosity as a result of molecular motion restriction imposed by the nanoparticles [175]. This effect is dependent on the state of dispersion of particles in the matrix. For example, in a study on PLA nanocomposites reinforced with CNC, it was found that for up to 2.5 wt% of CNC, the complex viscosity increased. However, further addition of CNC resulted in decrease in complex viscosity. This effect was attributed to severe agglomeration of CNCs at higher concentrations that resulted in relatively lower molecular entanglement density which, in turn, reduced the viscosity of the matrix.

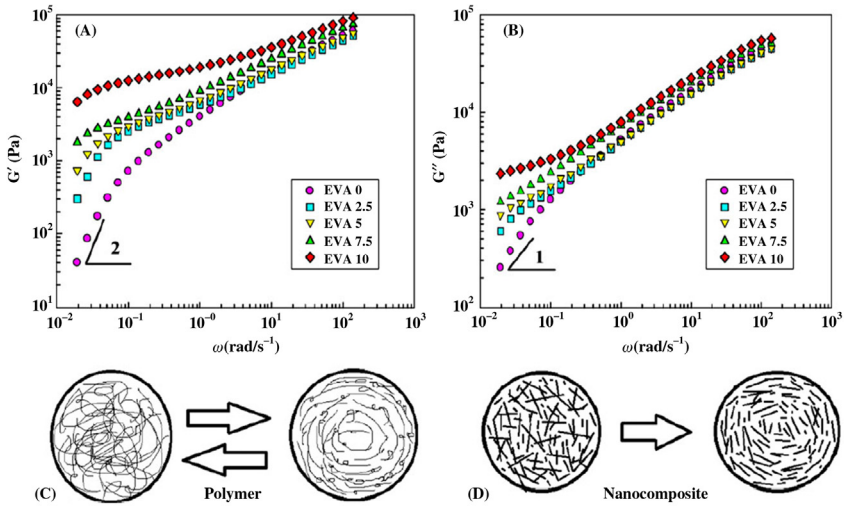

Figure 4.8 Variation of (A) storage and (B) loss modulus of EVA melt with CNC concentration. Shear-induced orientation of (C) polymer chains and (D) CNC nanoparticles. Reproduced from Ref. [170] with permission from Springer.

The complex viscosity CNC/polymer nanocomposites show strong dependence on frequency and the nanocomposites exhibit shear-thinning behavior. While the neat polymer matrix shows no dependence of complex viscosity on angular frequency at low-frequency values as evidenced by and a plateau in the complex viscosity versus frequency plot, addition of CNC was shown to significantly promote non-Newtonian behavior and increase of viscosity at low-frequency ranges which is related with the nanostructure signature [176]. In addition, surface chemistry and interfacial compatibility with the matrix play a major role in rheological behavior of CNC nanocomposites. Application of polyaniline-*g*-CNC was found to develop non-Newtonian shear-thinning behavior in PU matrix [177] at low concentrations unlike the nonmodified CNC. It was suggested that the liquid−solid transition is significantly promoted through the compatibility of the surface PANI layer with the PU matrix.

Goffin *et al*. [103] studied the role of PCL-*g*-CNC in a PCL matrix through rheological characterization. It was seen that above 8% of the modified CNC, a network-like structure formed within the matrix that enhanced the elasticity and solid-like behavior of the matrix. This finding is ascribed to the coentanglement of the surface-grafted PCL layer with the PCL matrix which promoted the stress transfer to particles and imposed significant molecular motion restriction on the matrix.

4.5.4 Gas barrier properties

There has been an increasing demand in plastic packaging industry for ecofriendly alternatives of petroleum-based polymers for use in packaging materials. The major requirement in this application is high gas barrier property of the film. The application of CNCs in gas barrier membranes has been reported in a number of research papers in the literature to improve the gas barrier property of cellulose-based thin films. In one of the early studies on PVOH membranes reinforced with CNCs [81], it was observed that the CNC effectively reduced the gas permeation flux while it allowed the moisture to pass through. Surface modification of CNC by acetylation resulted in better dispersion in PVA matrix and significantly improved the barrier properties. Fortunati *et al.* [178] dispersed CNCs in a PLA matrix with the aid of surfactant and observed 34% reduction in water permeability with only 1% of surfactant-modified CNC. They also reported good oxygen barrier property for 1 and 5 wt% of unmodified and modified CNCs dispersed in the PLA matrix. Khan *et al.* [123] 27% decrease in water vapor permeability in a chitosan/CNC biodegradable films containing 5 wt% of CNC. Li *et al*. [124] developed chitosan/CNC multilayered thin films on PET substrate by LbL assembly technique and observed surprisingly low oxygen permeability value of 0.043 $cm^3\ \mu m\ m^{-2}\ 24\ h^{-1}\ kPa^{-1}$, which is close to that of EVOH copolymers, under dry conditions. In other similar studies, promising reduction in water vapor transmission rate for carboxymethyl cellulose [179] and plasticized starch films [180] by addition of CNCs were reported. In a study on PCL nanocomposites reinforced with CNCs [181], it was reported that the reduction in rate of water vapor permeation is due to the reduction in gas diffusion because of relatively longer tortuous travel path of the water molecules through the rod-shaped cellulose whiskers. It should however be mentioned that the development of the CNC network is likely to be a most important

requirement for superior barrier property as the comparison study of microfibrillated cellulose (MFC) and cellulose whiskers for their barrier property [182] showed that the MFC had better barrier property due to the network-like structure and entanglement of cellulose filaments, while CNC had much higher porosity to allow the gas molecule passage.

4.6 Conclusion and future perspective

The plethora of research advancements and scientific discoveries over the past decade in the investigation of physics and chemistry of CNCs reveal a number of potential uses of green hybrid polymer/CNC nanocomposites with enhanced benefits. This perspective is strongly motivated by research efforts in the scientific and industrial communities to develop sustainable materials from biorenewable resources to address increasing environmental legislations and concerns with conventional petroleum-based products. One of the challenges in the development of polymer/CNC nanocomposites materials is the problem associated with large scale industrial production. This drawback is being addressed by recent major research and development initiatives such as the establishment of CNC production pilot plants in the US Forest Product Laboratory that is capable of producing large quantities of CNCs as a first step toward commercialization of CNC production facilities.

From a scientific research perspective, there are two major future directions to be explored. One area is the application and utilization of CNCs as functional additives for polymer nanocomposites as composite reinforcements, rheological modifiers, and gas barrier additives. The second area is the development of reliable strategies to improve the dispersion of the CNCs in polymer matrices using scalable processing methods such as extrusion and injection molding to afford novel functional materials and devices using CNCs in the field of polymeric electronics like recyclable and reusable solar cells [183], green low-cost nanopaper flexible electronic substrates [184,185], and biomedical applications such as drug delivery [186], injectable scaffolds and tissue engineering [187], and other pharmaceutical applications [188]. It is hoped that this chapter will provide a basis for further development of functional polymer/CNC nanocomposites for a number of uses in existing and new applications.

Acknowledgments

This work was supported by the US National Science Foundation Division of Civil, Mechanical, and Manufacturing Innovation through CMMI-1161292 grant award and Office of International and Integrative Activities through IIA-1346898. The research work of J.U.O's former graduate students and postdocs and funding by the US Department of State, the French Ministry of Higher Education and Research, and the Franco-American Commission of his Fulbright-Tocqueville Distinguished Chair award in Engineering at the University of Lyon 1 are gratefully acknowledged. We are indebted to our collaborators, with whom we had the privilege of working on projects cited in this chapter.

References

[1] Hubbe MA, et al. Cellulosic nanocomposites: a review. BioResources 2008;3(3):929–80.

[2] Rojas J, Bedoya M, Ciro Y. Current trends in the production of cellulose nanoparticles and nanocomposites for biomedical applications. In: Poletto M, Ornaghi HL, editors. Cellulose – Fundamental Aspects and Current Trends. Rijeka: InTech; 2015.

[3] Spence K, Habibi Y, Dufresne A. Nanocellulose-based composites, in cellulose fibers: bio- and nano-polymer composites. Berlin, Heidelberg: Springer; 2011. p. 179–213.

[4] Atalla RH, et al. *Structures of plant cell wall celluloses*. Biomass recalcitrance: deconstructing the plant cell wall for bioenergy. Oxford: Wiley-Blackwell; 2008. p. 188–212.

[5] Habibi Y, Lucia LA, Rojas OJ. Cellulose nanocrystals: chemistry, self-assembly, and applications. Chem Rev 2010;110(6):3479–500.

[6] Moon RJ, et al. Cellulose nanomaterials review: structure, properties and nanocomposites. Chem Soc Rev 2011;40(7):3941–94.

[7] Kaushik A, Singh M, Verma G. Green nanocomposites based on thermoplastic starch and steam exploded cellulose nanofibrils from wheat straw. Carbohydr Polym 2010;82(2):337–45.

[8] Sacui IA, et al. Comparison of the properties of cellulose nanocrystals and cellulose nanofibrils isolated from bacteria, tunicate, and wood processed using acid, enzymatic, mechanical, and oxidative methods. ACS Appl Mater Interfaces 2014;6(9):6127–38.

[9] Jonas R, Farah LF. Production and application of microbial cellulose. Polym Degradation Stability 1998;59(1):101–6.

[10] George J, Ramana K, Bawa A. *Bacterial cellulose nanocrystals exhibiting high thermal stability and their polymer nanocomposites*. Int J Biol Macromol 2011;48(1):50–7.

[11] Beck-Candanedo S, Roman M, Gray DG. Effect of reaction conditions on the properties and behavior of wood cellulose nanocrystal suspensions. Biomacromol 2005;6(2):1048–54.

[12] Saïd Azizi Samir MA, et al. Tangling effect in fibrillated cellulose reinforced nanocomposites. Macromolecules 2004;37(11):4313–16.

[13] Yue Y, et al. Comparative properties of cellulose nano-crystals from native and mercerized cotton fibers. Cellulose 2012;19(4):1173–87.

[14] Cao X, Dong H, Li CM. New nanocomposite materials reinforced with flax cellulose nanocrystals in waterborne polyurethane. Biomacromolecules 2007;8(3):899–904.

[15] Garcia de Rodriguez LN, Thielemans W, Dufresne A. Sisal cellulose whiskers reinforced polyvinyl acetate nanocomposites. Cellulose 2006;13(3):261–70.

[16] Habibi Y, et al. Langmuir–Blodgett films of cellulose nanocrystals: preparation and characterization. J Colloid Interface Sci 2007;316(2):388–97.

[17] Wang B, Sain M, Oksman K. Study of structural morphology of hemp fiber from the micro to the nanoscale. Appl Composite Mater 2007;14(2):89–103.

[18] Brinchi L, et al. Production of nanocrystalline cellulose from lignocellulosic biomass: technology and applications. Carbohydr Polym 2013;94(1):154–69.

[19] De Souza Lima M, et al. Translational and rotational dynamics of rodlike cellulose whiskers. Langmuir 2003;19(1):24–9.

[20] Habibi Y, et al. Bionanocomposites based on poly (ε-caprolactone)-grafted cellulose nanocrystals by ring-opening polymerization. J Mater Chem 2008;18(41):5002–10.

[21] Grunert M, Winter WT. Nanocomposites of cellulose acetate butyrate reinforced with cellulose nanocrystals. J Polym Environ 2002;10(1):27–30.

[22] Kargarzadeh H, et al. Effects of hydrolysis conditions on the morphology, crystallinity, and thermal stability of cellulose nanocrystals extracted from kenaf bast fibers. Cellulose 2012;19(3):855–66.
[23] Dong XM, Revol J-F, Gray DG. Effect of microcrystallite preparation conditions on the formation of colloid crystals of cellulose. Cellulose 1998;5(1):19–32.
[24] Bondeson D, Mathew A, Oksman K. Optimization of the isolation of nanocrystals from microcrystalline cellulose by acid hydrolysis. Cellulose 2006;13(2):171–80.
[25] Hamad WY, Hu TQ. Structure–process–yield interrelations in nanocrystalline cellulose extraction. Can J Chem Eng 2010;88(3):392–402.
[26] Elazzouzi-Hafraoui S, et al. The shape and size distribution of crystalline nanoparticles prepared by acid hydrolysis of native cellulose. Biomacromolecules 2007;9(1):57–65.
[27] Bai W, Holbery J, Li K. A technique for production of nanocrystalline cellulose with a narrow size distribution. Cellulose 2009;16(3):455–65.
[28] de Souza Lima MM, Borsali R. Static and dynamic light scattering from polyelectrolyte microcrystal cellulose. Langmuir 2002;18(4):992–6.
[29] Yu H, et al. Facile extraction of thermally stable cellulose nanocrystals with a high yield of 93% through hydrochloric acid hydrolysis under hydrothermal conditions. J Mater Chem A 2013;1(12):3938–44.
[30] Araki J, et al. Flow properties of microcrystalline cellulose suspension prepared by acid treatment of native cellulose. Colloids Surf A: Physicochem Eng Aspects 1998;142 (1):75–82.
[31] Rusli R, et al. Stress transfer in cellulose nanowhisker composites—influence of whisker aspect ratio and surface charge. Biomacromolecules 2011;12(4):1363–9.
[32] Wang N, Ding E, Cheng R. Preparation and liquid crystalline properties of spherical cellulose nanocrystals. Langmuir 2008;24(1):5–8.
[33] Wang N, Ding E, Cheng R. Thermal degradation behaviors of spherical cellulose nanocrystals with sulfate groups. Polymer 2007;48(12):3486–93.
[34] Camarero Espinosa S, et al. Isolation of thermally stable cellulose nanocrystals by phosphoric acid hydrolysis. Biomacromolecules 2013;14(4):1223–30.
[35] Tang Y, et al. Extraction of cellulose nano-crystals from old corrugated container fiber using phosphoric acid and enzymatic hydrolysis followed by sonication. Carbohydr Polym 2015;125:360–6.
[36] Sadeghifar H, et al. Production of cellulose nanocrystals using hydrobromic acid and click reactions on their surface. J Mater Sci 2011;46(22):7344–55.
[37] Iwamoto S, Nakagaito A, Yano H. Nano-fibrillation of pulp fibers for the processing of transparent nanocomposites. Appl Phys A 2007;89(2):461–6.
[38] Chakraborty A, Sain M, Kortschot M. Cellulose microfibrils: a novel method of preparation using high shear refining and cryocrushing. Holzforschung 2005;59(1):102–7.
[39] Stelte W, Sanadi AR. Preparation and characterization of cellulose nanofibers from two commercial hardwood and softwood pulps. Ind Eng Chem Res 2009;48(24):11211–19.
[40] Saito T, et al. Individualization of nano-sized plant cellulose fibrils by direct surface carboxylation using TEMPO catalyst under neutral conditions. Biomacromolecules 2009;10(7):1992–6.
[41] Cherian BM, et al. Isolation of nanocellulose from pineapple leaf fibres by steam explosion. Carbohydr Polym 2010;81(3):720–5.
[42] Green O, et al. The design of polymeric ionic liquids for the preparation of functional materials. Polym Rev 2009;49(4):339–60.
[43] Marsh K, Boxall J, Lichtenthaler R. Room temperature ionic liquids and their mixtures—a review. Fluid Phase Equilibria 2004;219(1):93–8.

[44] Kilpeläinen I, et al. Dissolution of wood in ionic liquids. J Agric Food Chem 2007;55 (22):9142–8.
[45] Li C, Zhao ZK. Efficient acid-catalyzed hydrolysis of cellulose in ionic liquid. Adv Synth Catal 2007;349(11–12):1847–50.
[46] Man Z, et al. Preparation of cellulose nanocrystals using an ionic liquid. J Polym Environ 2011;19(3):726–31.
[47] Tan XY, Hamid SBA, Lai CW. Preparation of high crystallinity cellulose nanocrystals (CNCs) by ionic liquid solvolysis. Biomass Bioenergy 2015;81:584–91.
[48] Abushammala H, Krossing I, Laborie M-P. Ionic liquid-mediated technology to produce cellulose nanocrystals directly from wood. Carbohydr Polym 2015;134:609–16.
[49] Brandt A, et al. The effect of the ionic liquid anion in the pretreatment of pine wood chips. Green Chem 2010;12(4):672–9.
[50] Favier V, et al. Nanocomposite materials from latex and cellulose whiskers. Polym Adv Technol 1995;6(5):351–5.
[51] Gindl W, Keckes J. All-cellulose nanocomposite. Polymer 2005;46(23):10221–5.
[52] Gardner DJ, et al. Adhesion and surface issues in cellulose and nanocellulose. J Adhes Sci Technol 2008;22(5–6):545–67.
[53] Salas C, et al. Nanocellulose properties and applications in colloids and interfaces. Curr Opin Colloid Interface Sci 2014;19(5):383–96.
[54] Li Z, Renneckar S, Barone JR. Nanocomposites prepared by in situ enzymatic polymerization of phenol with TEMPO-oxidized nanocellulose. Cellulose 2010;17(1): 57–68.
[55] Besbes I, Alila S, Boufi S. Nanofibrillated cellulose from TEMPO-oxidized eucalyptus fibres: effect of the carboxyl content. Carbohydr Polym 2011;84(3):975–83.
[56] De Nooy A, Besemer A, Van Bekkum H. Highly selective TEMPO mediated oxidation of primary alcohol groups in polysaccharides. Recueil des Travaux Chimiques des Pays-Bas 1994;113(3):165–6.
[57] Habibi Y, Chanzy H, Vignon MR. TEMPO-mediated surface oxidation of cellulose whiskers. Cellulose 2006;13(6):679–87.
[58] Benkaddour A, et al. Grafting of polycaprolactone on oxidized nanocelluloses by click chemistry. Nanomaterials 2013;3(1):141–57.
[59] Salon M-CB, et al. Silane adsorption onto cellulose fibers: hydrolysis and condensation reactions. J Colloid Interface Sci 2005;289(1):249–61.
[60] Huda MS, et al. Effect of fiber surface-treatments on the properties of laminated biocomposites from poly (lactic acid)(PLA) and kenaf fibers. Composites Sci Technol 2008;68(2):424–32.
[61] Xie Y, et al. Silane coupling agents used for natural fiber/polymer composites: a review. Composites A: Appl Sci Manuf 2010;41(7):806–19.
[62] Goussé C, et al. Stable suspensions of partially silylated cellulose whiskers dispersed in organic solvents. Polymer 2002;43(9):2645–51.
[63] Yu H-Y, et al. Silylation of cellulose nanocrystals and their reinforcement of commercial silicone rubber. J Nanopart Res 2015;17(9):1–13.
[64] Raquez JM, et al. Surface-modification of cellulose nanowhiskers and their use as nanoreinforcers into polylactide: a sustainably-integrated approach. Composites Sci Technol 2012;72(5):544–9.
[65] Yu X, et al. Adsorption of heavy metal ions from aqueous solution by carboxylated cellulose nanocrystals. J Environ Sci 2013;25(5):933–43.
[66] Yuan H, et al. Surface acylation of cellulose whiskers by drying aqueous emulsion. Biomacromolecules 2006;7(3):696–700.

[67] Sassi J-F, Chanzy H. Ultrastructural aspects of the acetylation of cellulose. Cellulose 1995;2(2):111–27.
[68] Carlmark A, Larsson E, Malmström E. Grafting of cellulose by ring-opening polymerisation – a review. Eur Polym J 2012;48(10):1646–59.
[69] Hafrén J, Córdova A. Direct organocatalytic polymerization from cellulose fibers. Macromol Rapid Commun 2005;26(2):82–6.
[70] Carlsson L, et al. Surface characteristics of cellulose nanoparticles grafted by surface-initiated ring-opening polymerization of ε-caprolactone. Cellulose 2015;22(2): 1063–74.
[71] Lin N, et al. Effects of polymer-grafted natural nanocrystals on the structure and mechanical properties of poly (lactic acid): a case of cellulose whisker-graft-polycaprolactone. J Appl Polym Sci 2009;113(5):3417–25.
[72] Morandi G, Heath L, Thielemans W. Cellulose nanocrystals grafted with polystyrene chains through surface-initiated atom transfer radical polymerization (SI-ATRP). Langmuir 2009;25(14):8280–6.
[73] Zeinali E, Haddadi-Asl V, Roghani-Mamaqani H. Nanocrystalline cellulose grafted random copolymers of *N*-isopropylacrylamide and acrylic acid synthesized by RAFT polymerization: effect of different acrylic acid contents on LCST behavior. RSC Adv 2014;4(59):31428–42.
[74] de Souza Lima MM, Borsali R. Rodlike cellulose microcrystals: structure, properties, and applications. Macromol Rapid Commun 2004;25(7):771–87.
[75] Gradwell SE, et al. Surface modification of cellulose fibers: towards wood composites by biomimetics. Comptes Rendus Biol 2004;327(9–10):945–53.
[76] Hu Z, et al. Surfactant-enhanced cellulose nanocrystal Pickering emulsions. J Colloid Interface Sci 2015;439:139–48.
[77] Salajková M, Berglund LA, Zhou Q. Hydrophobic cellulose nanocrystals modified with quaternary ammonium salts. J Mater Chem 2012;22(37):19798–805.
[78] Rojas OJ, Montero GA, Habibi Y. Electrospun nanocomposites from polystyrene loaded with cellulose nanowhiskers. J Appl Polym Sci 2009;113(2):927–35.
[79] Kim J, et al. Dispersion of cellulose crystallites by nonionic surfactants in a hydrophobic polymer matrix. Polym Eng Sci 2009;49(10):2054–61.
[80] Dufresne A. Processing of polymer nanocomposites reinforced with polysaccharide nanocrystals. Molecules 2010;15(6):4111–28.
[81] Paralikar SA, Simonsen J, Lombardi J. Poly(vinyl alcohol)/cellulose nanocrystal barrier membranes. J Membr Sci 2008;320(1–2):248–58.
[82] Azizi Samir MAS, et al. Nanocomposite polymer electrolytes based on poly(oxyethylene) and cellulose nanocrystals. J Phys Chem B 2004;108(30):10845–52.
[83] Azizi Samir MAS, et al. Preparation of cellulose whiskers reinforced nanocomposites from an organic medium suspension. Macromolecules 2004;37(4):1386–93.
[84] van den Berg O, Capadona JR, Weder C. Preparation of homogeneous dispersions of tunicate cellulose whiskers in organic solvents. Biomacromolecules 2007;8(4):1353–7.
[85] Marcovich N, et al. Cellulose micro/nanocrystals reinforced polyurethane. J Mater Res 2006;21(04):870–81.
[86] Liu H, et al. Fabrication and properties of transparent polymethylmethacrylate/cellulose nanocrystals composites. Bioresour Technol 2010;101(14):5685–92.
[87] Capadona JR, et al. A versatile approach for the processing of polymer nanocomposites with self-assembled nanofibre templates. Nat Nanotechnol 2007;2(12):765–9.
[88] Capadona JR, et al. Polymer nanocomposites with nanowhiskers isolated from microcrystalline cellulose. Biomacromolecules 2009;10(4):712–16.

[89] Wang D, et al. Transparent bionanocomposites with improved properties from poly (propylene carbonate)(PPC) and cellulose nanowhiskers (CNWs). Composites Sci Technol 2013;85:83−9.
[90] Ljungberg N, et al. New nanocomposite materials reinforced with cellulose whiskers in atactic polypropylene: effect of surface and dispersion characteristics. Biomacromolecules 2005;6(5):2732−9.
[91] Cetin NS, et al. Acetylation of cellulose nanowhiskers with vinyl acetate under moderate conditions. Macromol Biosci 2009;9(10):997−1003.
[92] Berlioz S, et al. Gas-phase surface esterification of cellulose microfibrils and whiskers. Biomacromolecules 2009;10(8):2144−51.
[93] Ray SS, Okamoto M. Polymer/layered silicate nanocomposites: a review from preparation to processing. Prog Polym Sci 2003;28(11):1539−641.
[94] Junior de Menezes A, et al. Extrusion and characterization of functionalized cellulose whiskers reinforced polyethylene nanocomposites. Polymer 2009;50(19):4552−63.
[95] Ben Azouz K, et al. Simple method for the melt extrusion of a cellulose nanocrystal reinforced hydrophobic polymer. ACS Macro Lett 2011;1(1):236−40.
[96] Lee K-Y, et al. On the use of nanocellulose as reinforcement in polymer matrix composites. Composites Sci Technol 2014;105:15−27.
[97] Pandey JK, et al. Dispersion of nanocellulose (NC) in polypropylene (PP) and polyethylene (PE) matrix. In: Pandey KJ, et al., editors. Handbook of Polymer Nanocomposites. Processing, Performance and Application: Volume C: Polymer Nanocomposites of Cellulose Nanoparticles. Berlin, Heidelberg: Springer Berlin Heidelberg; 2015. p. 179−89.
[98] Lin N, Dufresne A. Physical and/or chemical compatibilization of extruded cellulose nanocrystal reinforced polystyrene nanocomposites. Macromolecules 2013;46(14):5570−83.
[99] Bondeson D, Oksman K. Dispersion and characteristics of surfactant modified cellulose whiskers nanocomposites. Composite Interfaces 2007;14(7−9):617−30.
[100] Oksman K, et al. Manufacturing process of cellulose whiskers/polylactic acid nanocomposites. Composites Sci Technol 2006;66(15):2776−84.
[101] Chazeau L, Cavaillé JY, Terech P. Mechanical behaviour above Tg of a plasticised PVC reinforced with cellulose whiskers; a SANS structural study. Polymer 1999;40 (19):5333−44.
[102] Jiang L, et al. Study of the poly(3-hydroxybutyrate-co-3-hydroxyvalerate)/cellulose nanowhisker composites prepared by solution casting and melt processing. J Composite Mater 2008;42(24):2629−45.
[103] Goffin AL, et al. Poly(ε-caprolactone) based nanocomposites reinforced by surface-grafted cellulose nanowhiskers via extrusion processing: morphology, rheology, and thermo-mechanical properties. Polymer 2011;52(7):1532−8.
[104] Karimi S, et al. A comparative study on characteristics of nanocellulose reinforced thermoplastic starch biofilms prepared with different techniques. Nordic Pulp Pap Res J 2014;29(1):41−5.
[105] Bondeson D, Oksman K. Polylactic acid/cellulose whisker nanocomposites modified by polyvinyl alcohol. Composites A: Appl Sci Manuf 2007;38(12):2486−92.
[106] Mathew AP, et al. The structure and mechanical properties of cellulose nanocomposites prepared by twin screw extrusion. In. ACS symposium series. Washington, DC: Oxford University Press; 2006.
[107] Goffin A-L, et al. From interfacial ring-opening polymerization to melt processing of cellulose nanowhisker-filled polylactide-based nanocomposites. Biomacromolecules 2011;12(7):2456−65.

[108] Kickelbick G. Hybrid materials: synthesis, characterization, and applications. Weinheim: John Wiley & Sons; 2007.
[109] Liu H, Laborie M-PG. Bio-based nanocomposites by in situ cure of phenolic prepolymers with cellulose whiskers. Cellulose 2011;18(3):619–30.
[110] Tang L, Weder C. Cellulose whisker/epoxy resin nanocomposites. ACS Appl Mater Interfaces 2010;2(4):1073–80.
[111] Li Y, Ren H, Ragauskas AJ. Rigid polyurethane foam/cellulose whisker nanocomposites: preparation, characterization, and properties. J Nanosci Nanotechnol 2011;11 (8):6904–11.
[112] Pei A, et al. Strong nanocomposite reinforcement effects in polyurethane elastomer with low volume fraction of cellulose nanocrystals. Macromolecules 2011;44(11): 4422–7.
[113] Cao X, Habibi Y, Lucia LA. One-pot polymerization, surface grafting, and processing of waterborne polyurethane-cellulose nanocrystal nanocomposites. J Mater Chem 2009;19(38):7137–45.
[114] Pranger LA, Nunnery GA, Tannenbaum R. Mechanism of the nanoparticle-catalyzed polymerization of furfuryl alcohol and the thermal and mechanical properties of the resulting nanocomposites. Composites B: Eng 2012;43(3):1139–46.
[115] Pranger L, Tannenbaum R. Biobased nanocomposites prepared by in situ polymerization of furfuryl alcohol with cellulose whiskers or montmorillonite clay. Macromolecules 2008;41(22):8682–7.
[116] Kashani Rahimi S, Otaigbe JU. Polyamide 6 nanocomposites incorporating cellulose nanocrystals prepared by in-situ ring opening polymerization: viscoelasticity, creep behavior, and melt rheological properties. Polym Eng Sci 2016;56(9):1045–60.
[117] Podsiadlo P, et al. Molecularly engineered nanocomposites: layer-by-layer assembly of cellulose nanocrystals. Biomacromolecules 2005;6(6):2914–18.
[118] Qin S, et al. Covalent cross-linked polymer/single-wall carbon nanotube multilayer films. Chem Mater 2005;17(8):2131–5.
[119] Olek M, et al. Layer-by-layer assembled composites from multiwall carbon nanotubes with different morphologies. Nano Lett 2004;4(10):1889–95.
[120] de Mesquita JP, Donnici CL, Pereira FV. Biobased nanocomposites from layer-by-layer assembly of cellulose nanowhiskers with chitosan. Biomacromolecules 2010;11 (2):473–80.
[121] Podsiadlo P, et al. Layer-by-layer assembled films of cellulose nanowires with antireflective properties. Langmuir 2007;23(15):7901–6.
[122] Cranston ED, Gray DG. Morphological and optical characterization of polyelectrolyte multilayers incorporating nanocrystalline cellulose. Biomacromolecules 2006;7(9): 2522–30.
[123] Khan A, et al. Mechanical and barrier properties of nanocrystalline cellulose reinforced chitosan based nanocomposite films. Carbohydr Polym 2012;90(4):1601–8.
[124] Li F, et al. Tunable green oxygen barrier through layer-by-layer self-assembly of chitosan and cellulose nanocrystals. Carbohydr Polym 2013;92(2):2128–34.
[125] de Mesquita JP, et al. Hybrid layer-by-layer assembly based on animal and vegetable structural materials: multilayered films of collagen and cellulose nanowhiskers. Soft Matter 2011;7(9):4405–13.
[126] Siqueira G, Bras J, Dufresne A. Cellulosic bionanocomposites: a review of preparation, properties and applications. Polymers 2010;2(4):728–65.
[127] Šturcová A, Davies GR, Eichhorn SJ. Elastic modulus and stress-transfer properties of tunicate cellulose whiskers. Biomacromolecules 2005;6(2):1055–61.

[128] Rusli R, Eichhorn SJ. Determination of the stiffness of cellulose nanowhiskers and the fiber-matrix interface in a nanocomposite using Raman spectroscopy. Appl Phys Lett 2008;93(3):033111.
[129] Lahiji RR, et al. Atomic force microscopy characterization of cellulose nanocrystals. Langmuir 2010;26(6):4480–8.
[130] Wagner R, Raman A, Moon R. Transverse elasticity of cellulose nanocrystals via atomic force microscopy. Cellulose 2010;7:27.
[131] Cao X, et al. Green composites reinforced with hemp nanocrystals in plasticized starch. J Appl Polym Sci 2008;109(6):3804–10.
[132] Shi Q, et al. Mechanical properties and in vitro degradation of electrospun bio-nanocomposite mats from PLA and cellulose nanocrystals. Carbohydr Polym 2012;90 (1):301–8.
[133] Lin N, et al. Poly(butylene succinate)-based biocomposites filled with polysaccharide nanocrystals: structure and properties. Polym Composites 2011;32(3):472–82.
[134] Ibrahim MM, El-Zawawy WK. Poly(vinyl alcohol)-cellulose and nanocellulose composites. Handbook of Polymer Nanocomposites. Processing, Performance and Application. Berlin, Heidelberg: Springer; 2015. p. 297–322.
[135] Fortunati E, et al. Processing of PLA nanocomposites with cellulose nanocrystals extracted from *Posidonia oceanica* waste: innovative reuse of coastal plant. Ind Crops Prod 2015;67:439–47.
[136] Anžlovar A, Huskić M, Žagar E. Modification of nanocrystalline cellulose for application as a reinforcing nanofiller in PMMA composites. Cellulose 2016;23(1):505–18.
[137] Zhang Z, et al. Poly(vinylidene fluoride)/cellulose nanocrystals composites: rheological, hydrophilicity, thermal and mechanical properties. Cellulose 2015;22 (4):2431–41.
[138] Seoane IT, et al. Development and characterization of bionanocomposites based on poly(3-hydroxybutyrate) and cellulose nanocrystals for packaging applications. Polym Int 2016;65(9):1046–53.
[139] Corrêa AC, et al. Obtaining nanocomposites of polyamide 6 and cellulose whiskers via extrusion and injection molding. Cellulose 2014;21(1):311–22.
[140] Peng J, et al. Water-assisted compounding of cellulose nanocrystals into polyamide 6 for use as a nucleating agent for microcellular foaming. Polymer 2016;84:158–66.
[141] Gao Z, et al. Biocompatible elastomer of waterborne polyurethane based on castor oil and polyethylene glycol with cellulose nanocrystals. Carbohydr Polym 2012;87 (3):2068–75.
[142] Bras J, et al. Mechanical, barrier, and biodegradability properties of bagasse cellulose whiskers reinforced natural rubber nanocomposites. Ind Crops Prod 2010;32(3): 627–33.
[143] Pan H, et al. Transparent epoxy acrylate resin nanocomposites reinforced with cellulose nanocrystals. Ind Eng Chem Res 2012;51(50):16326–32.
[144] Kargarzadeh H, et al. Cellulose nanocrystal: a promising toughening agent for unsaturated polyester nanocomposite. Polymer 2015;56:346–57.
[145] Islam MT, Alam MM, Zoccola M. Review on modification of nanocellulose for application in composites. Int J Innov Res Sci Eng Technol 2013;2(10):5444–51.
[146] Silvério HA, et al. Extraction and characterization of cellulose nanocrystals from corncob for application as reinforcing agent in nanocomposites. Ind Crops Prod 2013;44:427–36.
[147] Littunen K, et al. Network formation of nanofibrillated cellulose in solution blended poly(methyl methacrylate) composites. Carbohydr Polym 2013;91(1):183–90.

[148] Rebouillat S, Pla F. State of the art manufacturing and engineering of nanocellulose: a review of available data and industrial applications. J Biomater Nanobiotechnol 2013;4(2):165.
[149] Minelli M, et al. Investigation of mass transport properties of microfibrillated cellulose (MFC) films. J Membr Sci 2010;358(1−2):67−75.
[150] Halpin JC, Kardos JL. Moduli of crystalline polymers employing composite theory. J Appl Phys 1972;43(5):2235−41.
[151] Takayanagi M, Uemura S, Minami S. Application of equivalent model method to dynamic rheo-optical properties of crystalline polymer. J Polym Sci C: Polym Symp 1964;5(1):113−22.
[152] Ouali N, Cavaillé J, Perez J. Elastic, viscoelastic and plastic behavior of multiphase polymer blends. Plastics Rubber Composites Process Appl (UK) 1991;16(1):55−60.
[153] Roman M, Winter WT. Effect of sulfate groups from sulfuric acid hydrolysis on the thermal degradation behavior of bacterial cellulose. Biomacromolecules 2004;5 (5):1671−7.
[154] Liu H, et al. Properties of rosin-based waterborne polyurethanes/cellulose nanocrystals composites. Carbohydr Polym 2013;96(2):510−15.
[155] Huq T, et al. Nanocrystalline cellulose (NCC) reinforced alginate based biodegradable nanocomposite film. Carbohydr Polym 2012;90(4):1757−63.
[156] Hajji P, et al. Tensile behavior of nanocomposites from latex and cellulose whiskers. Polym Composites 1996;17(4):612−19.
[157] Chazeau L, et al. Viscoelastic properties of plasticized PVC reinforced with cellulose whiskers. J Appl Polym Sci 1999;71(11):1797−808.
[158] Bendahou A, Kaddami H, Dufresne A. Investigation on the effect of cellulosic nanoparticles' morphology on the properties of natural rubber based nanocomposites. Eur Polym J 2010;46(4):609−20.
[159] Lu Y, Weng L, Cao X. Biocomposites of plasticized starch reinforced with cellulose crystallites from cottonseed linter. Macromol Biosci 2005;5(11):1101−7.
[160] Mathew AP, Dufresne A. Morphological investigation of nanocomposites from sorbitol plasticized starch and tunicin whiskers. Biomacromolecules 2002;3(3):609−17.
[161] Habibi Y, Dufresne A. Highly filled bionanocomposites from functionalized polysaccharide nanocrystals. Biomacromolecules 2008;9(7):1974−80.
[162] Pei A, Zhou Q, Berglund LA. Functionalized cellulose nanocrystals as biobased nucleation agents in poly(l-lactide)(PLLA)−crystallization and mechanical property effects. Composites Sci Technol 2010;70(5):815−21.
[163] Gray DG. Transcrystallization of polypropylene at cellulose nanocrystal surfaces. Cellulose 2008;15(2):297−301.
[164] Han J, et al. Morphology, reversible phase crystallization, and thermal sensitive shape memory effect of cellulose whisker/SMPU nano-composites. J Appl Polym Sci 2012;123(2):749−62.
[165] Liu D, et al. Structure and rheology of nanocrystalline cellulose. Carbohydr Polym 2011;84(1):316−22.
[166] Hasani M, et al. Cationic surface functionalization of cellulose nanocrystals. Soft Matter 2008;4(11):2238−44.
[167] Shafiei-Sabet S, Hamad WY, Hatzikiriakos SG. Rheology of nanocrystalline cellulose aqueous suspensions. Langmuir 2012;28(49):17124−33.
[168] Cox W, Merz E. Correlation of dynamic and steady flow viscosities. J Polym Sci 1958;28(118):619−22.

[169] Ten E, et al. Effects of cellulose nanowhiskers on mechanical, dielectric, and rheological properties of poly(3-hydroxybutyrate-*co*-3-hydroxyvalerate)/cellulose nanowhisker composites. Ind Eng Chem Res 2012;51(7):2941−51.
[170] Mahi H, Rodrigue D. Linear and non-linear viscoelastic properties of ethylene vinyl acetate/nano-crystalline cellulose composites. Rheologica Acta 2012;51(2):127−42.
[171] Mendez J, et al. Bioinspired mechanically adaptive polymer nanocomposites with water-activated shape-memory effect. Macromolecules 2011;44(17):6827−35.
[172] Yang J, et al. Mechanical and viscoelastic properties of cellulose nanocrystals reinforced poly(ethylene glycol) nanocomposite hydrogels. ACS Appl Mater Interfaces 2013;5(8):3199−207.
[173] Cao X, et al. New nanocomposite materials reinforced with cellulose nanocrystals in nitrile rubber. Polym Test 2013;32(5):819−26.
[174] Dagnon KL, et al. Controlling the rate of water-induced switching in mechanically dynamic cellulose nanocrystal composites. Macromolecules 2013;46(20):8203−12.
[175] Krishnamoorti R, Yurekli K. Rheology of polymer layered silicate nanocomposites. Curr Opin Colloid Interface Sci 2001;6(5):464−70.
[176] Kamal MR, Khoshkava V. Effect of cellulose nanocrystals (CNC) on rheological and mechanical properties and crystallization behavior of PLA/CNC nanocomposites. Carbohydr Polym 2015;123:105−14.
[177] Auad ML, et al. Polyaniline-modified cellulose nanofibrils as reinforcement of a smart polyurethane. Polym Int 2011;60(5):743−50.
[178] Fortunati E, et al. Effects of modified cellulose nanocrystals on the barrier and migration properties of PLA nano-biocomposites. Carbohydr Polym 2012;90(2):948−56.
[179] Choi Y, Simonsen J. Cellulose nanocrystal-filled carboxymethyl cellulose nanocomposites. J Nanosci Nanotechnol 2006;6(3):633−9.
[180] Chang PR, et al. Preparation and properties of glycerol plasticized-starch (GPS)/cellulose nanoparticle (CN) composites. Carbohydr Polym 2010;79(2):301−5.
[181] Follain N, et al. Water transport properties of bio-nanocomposites reinforced by Luffa cylindrica cellulose nanocrystals. J Membr Sci 2013;427:218−29.
[182] Belbekhouche S, et al. Water sorption behavior and gas barrier properties of cellulose whiskers and microfibrils films. Carbohydr Polym 2011;83(4):1740−8.
[183] Zhou Y, et al. Recyclable organic solar cells on cellulose nanocrystal substrates. Sci Rep 2013;3:1536.
[184] Lizundia E, et al. Cu-coated cellulose nanopaper for green and low-cost electronics. Cellulose 2016;23(3):1997−2010.
[185] Xu X, et al. Highly transparent, low-haze, hybrid cellulose nanopaper as electrodes for flexible electronics. Nanoscale 2016;8(24):12294−306.
[186] Ntoutoume GMN, et al. Development of curcumin−cyclodextrin/cellulose nanocrystals complexes: New anticancer drug delivery systems. Bioorg Med Chem Lett 2016;26(3):941−5.
[187] Wang K, Nune K, Misra R. The functional response of alginate-gelatin-nanocrystalline cellulose injectable hydrogels toward delivery of cells and bioactive molecules. Acta Biomater 2016;36:143−51.
[188] Song, Y.K., et al. NanoCrystalline cellulose, an environmental friendly nanoparticle for pharmaceutical application − a quick study. in MATEC Web of Conferences. 2016. EDP Sciences.